REPORT DOCUMENTATION PAGE

Form Approved OMB No. 0704-0188

Public reporting burden for this collection of information is estimated to average 1 hour per response, including the time for reviewing instructions, searching existing data sources, gathering and maintaining the data needed, and completing and reviewing the collection of information. Send comments regarding this burden estimate or any other aspect of this collection of information, including suggestions for reducing this burden to Washington Headquarters Services, Directorate for Information Operations and Reports, 1215 Jefferson Davis Highway, Suite 1204, Arlington, VA 22202-4302, and to the Office of Management and Budget, Paperwork Reduction Project (0704-0188), Washington, DC 20503.

1. AGENCY USE ONLY (Leave blank)	2. REPORT DATE	3. REPORT TYPE AND DATES COVERED
	1997	Final Report

4. TITLE AND SUBTITLE

Experimental Investigation Of A Possibility Of Application Of A Microwave Streamer Gas Discharge For Ignition Of Fuel In A Jet Engine

5. FUNDING NUMBERS

F6170897W0009

6. AUTHOR(S)

Dr. Elksei Ershov

7. PERFORMING ORGANIZATION NAME(S) AND ADDRESS(ES)

Moscow State University
Moscow 119899
Russia

8. PERFORMING ORGANIZATION REPORT NUMBER

N/A

9. SPONSORING/MONITORING AGENCY NAME(S) AND ADDRESS(ES)

EOARD
PSC 802 BOX 14
FPO 09499-0200

10. SPONSORING/MONITORING AGENCY REPORT NUMBER

SPC 97-4003

11. SUPPLEMENTARY NOTES

12a. DISTRIBUTION/AVAILABILITY STATEMENT

Approved for public release; distribution is unlimited.

12b. DISTRIBUTION CODE

A

13. ABSTRACT (Maximum 200 words)

This report results from a contract tasking Moscow State University as follows: The contractor will investigate of a possibility of application of a microwave streamer gas discharge for ignition of fuel in a jet engine as described in his proposal dated 14 Jun 96, with the exception that you will be required to purchase the equipment yourself.

DTIC QUALITY INSPECTED 7

14. SUBJECT TERMS

High Power Microwaves

15. NUMBER OF PAGES

77

16. PRICE CODE

N/A

17. SECURITY CLASSIFICATION OF REPORT	18. SECURITY CLASSIFICATION OF THIS PAGE	19, SECURITY CLASSIFICATION OF ABSTRACT	20. LIMITATION OF ABSTRACT
UNCLASSIFIED	UNCLASSIFIED	UNCLASSIFIED	UL

NSN 7540-01-280-5500

Standard Form 298 (Rev. 2-89)
Prescribed by ANSI Std. 239-18
298-102

FINAL REPORT

SPECIAL PROJECT SPC-97-4003

EXPERIMENTAL INVESTIGATION

OF A POSSIBILITY OF APPLICATION

OF A MICROWAVE STREAMER GAS DISCHARGE

FOR IGNITION OF FUEL IN A JET ENGINE

By
Dr. Elksei Ershov
Moscow State Univeristy
Moscow, Russia

CONTENTS

1. Introduction

One of the problems arising at development of a jet engine for a hypersonic plane is bound with ignition of fuel in such engine. With growth of a flow velocity, flow tubes of fuel and air practically do not mix up. In this case at local ignition of fuel it is difficult to provide its ignition in the whole cross section of the combustion chamber.

This problem can be solved with use of a microwave discharge in a focus of an electromagnetic beam. Such a discharge can be created at once in a considerable volume of a combustible mixture. However, for ignition of freely localized electrodeless microwave discharge at high gas pressure there are required rather high levels of microwave energy flux density in the beam S_o. For example, at air pressure $p = 760$ Torr the breakdown takes place at $S_o > S^* \cong 10^6$ W/cm^2. To achieve such levels of S_o, there are required powerful microwave generators (even in case of maximal possible focusing of the beam). For the previous example at wavelength of microwave radiation $\lambda = 4$ cm the power of the electromagnetic beam should be not less than 10 MW.

However, preliminary researches of the MW gas discharges in focused microwave beams of centimeter and decimeter ranges of wavelengths have shown, that under certain experimental conditions a streamer regime of microwave discharges takes place. A local initiation of such a discharge can be provided by special facilities. Then the streamer microwave discharge can spread in a considerable volume of the microwave beam. For such a case the level of S_o can be essentially less than the critical level of breakdown S^* (subcritical microwave discharge).

Thus, ignition of fuel in a supersonic engine with use of such an initiated streamer subcritical microwave discharge in a beam looks advantageous, as it

makes it possible to provide ignition of considerable volumes at tolerable requirements on energy level of microwave generators.

In the present report, results of our experimental research of the initiated subcritical streamer microwave discharges in a focused beam are presented. Physics of such a discharge is not known well, that's why in these researches its general properties are primarily studied, comparatively simply optical methods are used.

The experiments have shown, that such discharge passes several sequent stages. Basic physical factors which determine the discharge properties at these stages are considered in the report. Results of experiments with the initiated streamer discharges in various gases are presented. Physical features of the subcritical microwave streamer at initial stage of its development, which have been revealed experimentally, are also studied theoretically. Some formulae useful for estimates of possibility of practical implementation of this type of microwave discharge for ignition of fuel in a supersonic jet engine are given. A possible draft schematic diagram of an ignition system on base of MW discharge is suggested. Several possible directions of the further R&D are pointed out.

2. Experimantal Installations and Diagnostics Methods

2.1 Installation I

The scheme of the experimental installation is shown on Fig.1. Its photo frame is shown on Fig.2. The installation is universal. It contains a set of equipment which makes it possible to change experimental conditions in a very wide scale. That is why its units have considerable sizes. A specialized on board system of MW ignition may be made much smaller.
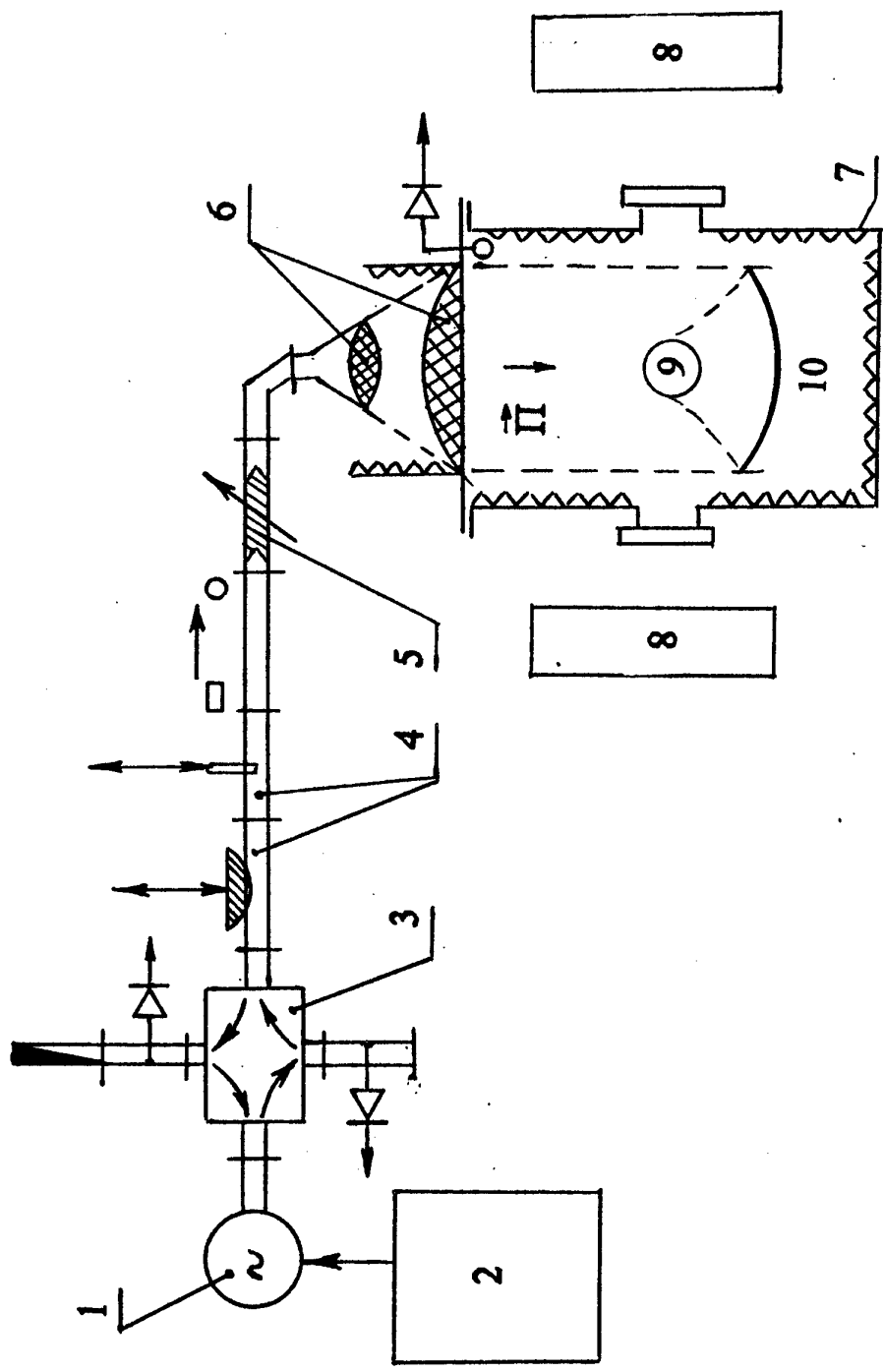
Рис.1 Schematic diagram of the installation

1 – MW source; 2 - modulator; 3 - circulator; 4 - attenuator; 5 - polarizer; 6 – lens system; 7 – vacuum-tight chamber; 8 – diagnostic equipment; 9 – discharge region; 10 – focusing mirror

Fig.2. Appearance of the installation

This installation can be used for researches of microwave discharges of different types (diffuse, streamer, resonant and cumulative regimes, see, for example, [3]) which are either freely localized in wave beams [1], or initiated by special facilities [2]. On this installation there had been studied: interaction of gas dynamical perturbations with plasma of microwave discharges, an opportunity of application of a microwave pinch in powerful installations for controlled fusion, etc.

The installation consists of a microwave power source, a vacuum chamber, a set of devices which provide the microwave radiation transport from the source to the chamber, focusing elements, and a set of diagnostic equipment.

A basic element of the microwave power source is a pulsed magnetron generator. Its power supply is provided by a modulator (see Fig.3) based on a partial discharge of a storage capacitor. The maximal pulsed power P of the magnetron is about 10^7 W. The microwave wavelength $\lambda = 8,5$ cm. The modulator generates rectangular microwave pulses, it provides discrete adjustment of their duration τ_p from 4 up to 40 µs with a 4 µs step. The maximal repetition frequency of the pulses is 1 Hz. At the present research, single pulses were used. Magnetron output is a rectangular 72x34 mm^2 waveguide.

The vacuum chamber (see Fig.4 and 5) consists of two basic parts.

The first part is a stationary metal cylinder with a huge (630mm in diameter) polystyrene lens in its butt end (see Fig.1), through which the microwave radiation enters the chamber. On the periphery there are located vacuum MW and high voltage sockets, through which the information input and output is made. At the internal part of the cylinder, four aluminum cores (1600 mm long, and 40 mm in diameter) are screwed normally to it and in regular intervals on a diameter of 680 mm. Various stationary equipment (for example, a focusing mirror, microwave absorbers, see Fig.1) can be fixed on them.
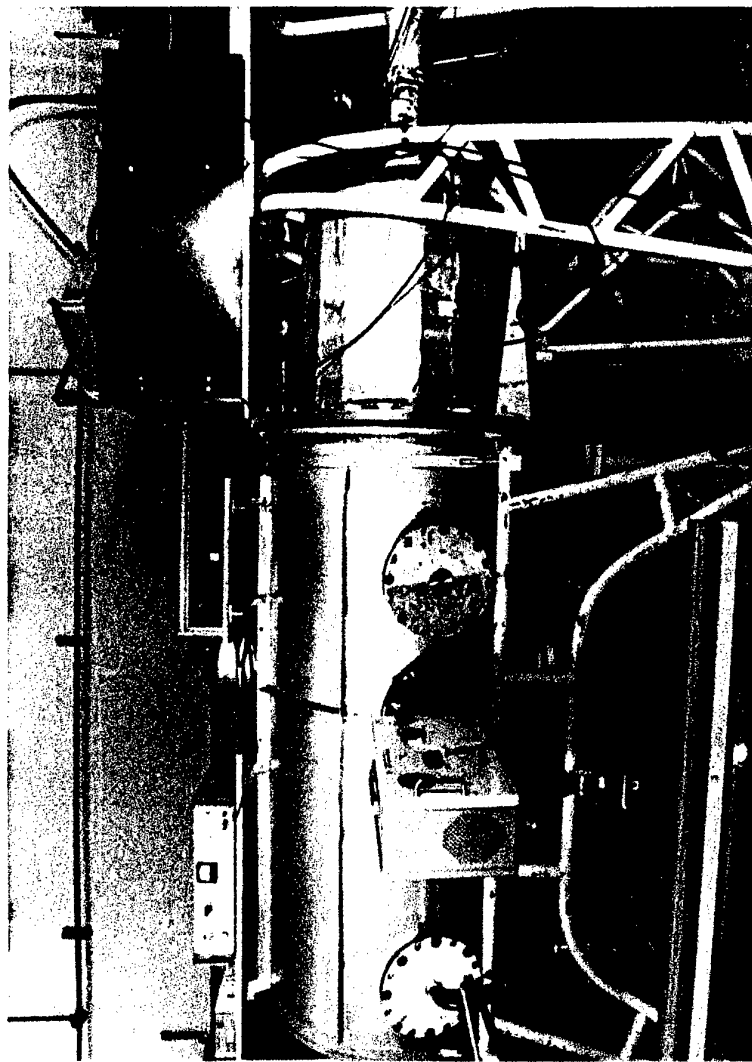
Fig.3. Modulator
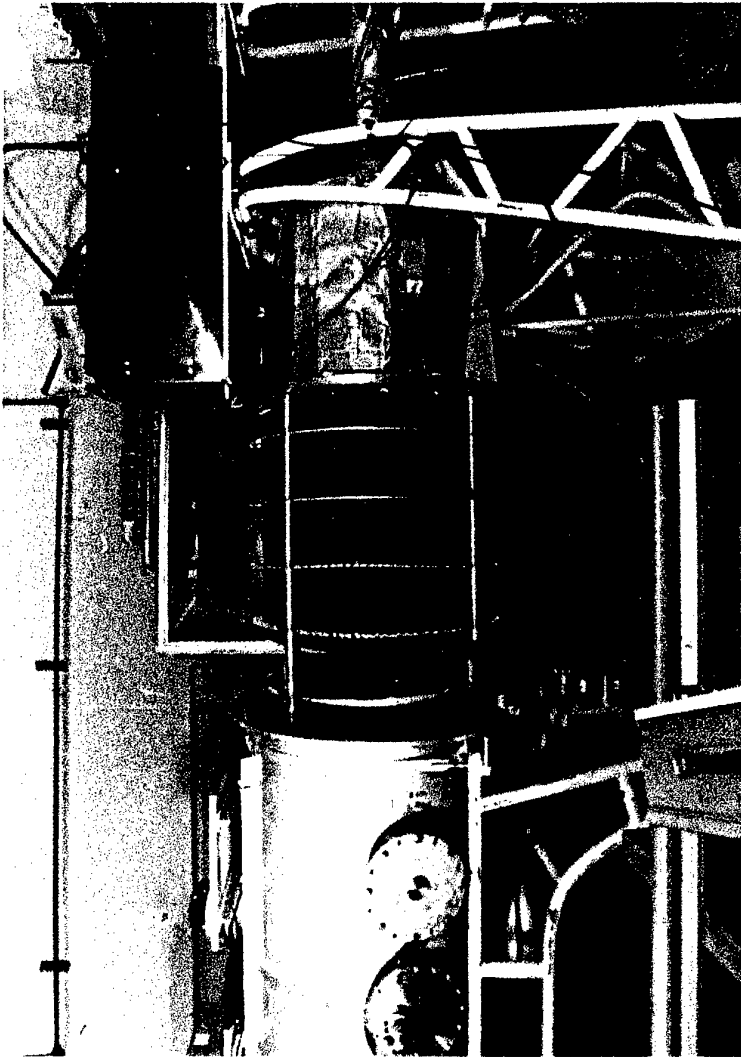
Fig.4. Vacuum-tight chamber

Fig.5. Vacuum-tight chamber - open

The second part of the chamber is a stainless steel cylinder (∅800×1700 mm) which is coaxial with the first part, and can be bolted to it. The second part is fixed to a wheel carriage, it can be rolled away to open the internal volume of the chamber to provide a convenient access.

The vacuum chamber has four windows. Three of them have 200 mm in diameter and one (looking down) has a 400 mm diameter. On the windows there can be fixed 20 mm thick optical glass plates, or organic glass water filled illuminators (for visual supervision and diagnostics of processes in the chamber), or metal plates with various experimental equipment (e.g., a supersonic nozzle).

A MW absorptive material coating of the internal surfaces of the vacuum chamber makes it free from microwave echo (20 dB level). Rubber gasket seals make the chamber water-proof.

The installation is equipped with a forevacuum pump which provides experiments in pressure range from 3 to 760 Torr. Pressure measurement is carried out by a pressure sensor with accuracy ±1,5 Torr. The chamber is tested down to $p_{min} = 10^{-5}$ Torr. In case of necessity, with use of the appropriate methods of pumping, the experimental range of pressure can be extended to p_{min}.

The described below experiments were carried out primarily in air. At consideration of use of other gases, it is specially mentioned in the text.

The microwave energy from magnetron is transported through the waveguide, which includes: a circulator, an attenuator, a polarizer, and a lens system. Before the polarizer the waveguide has a rectangular cross section 72x34 mm^2, with a transition to a round cross section (∅ 76 mm) at the very polarizer.

A ferrite polarization type circulator plays a role of a gate. It prevents the reflected wave to cause a failure of generation of the magnetron if a disturbance of the running wave mode regime takes place in the waveguide. To control the levels of direct and reflected waves, branching-off is used. The waveguide is equipped with two adjustable attenuators. The first attenuator is based on absorption of MW

radiation by water, it provides 5 times reduction of the electromagnetic wave amplitude. In the second one a controlled attenuation (up to 20 times of the field amplitude reduction) results from blocking the waveguide's cross section by a reflecting knife. The polarizer makes it possible to change the field polarization from linear (vertical) to circular. It contains a polystyrene 360 mm long and 12 mm thick plate, which can be turned around of the waveguide axis, without disassembling it. The polarization is checked an by electric field sensors situated at the output end of the waveguide. A conic diffuser with a polyethylene MW-transparent diverging lens ($\varnothing$ 25 mm) is attached to the waveguide. The axis of this lens coincides with the axis of the lens on the first part of the chamber, as shown in Fig.1. All waveguide system is sealed tight and is filled by the hexafluorated sulfur (SF_6) gas at an overpressure of 1 atmosphere.

The lens system of the installation consists of the lens on the target diffuser of the waveguide and the lens on the second part of the chamber, it provides input of the microwave radiation into the chamber as TEM mode wave with a flat phase front. The beam in the chamber is axisymmetric with approximately Gaussian distribution of intensity. A measured relative radial distribution of the microwave energy flow density on a distance from the lens z = 50 cm is exposed on Fig.6. In area close to the axis the dependence of S on the radial coordinate ρ can be approximated by the following expression:

$$S = S_{max} \exp(\rho/\rho_o)^2,$$

where ρ_o = 14 cm. At the experiments as a rule the magnetron worked in a regime with of a maximal field E_{max} = 1,3 10^3 V/cm (as measured on the axis at linear polarization and a completely opened attenuator), the corresponding maximal power flow being S_{max}=2 10^3 W/cm^2, and the total maximal microwave power input P = 1,2 10^6 W. Along the chamber axis the microwave beam is approximately homogeneous (on a level of 0,8).
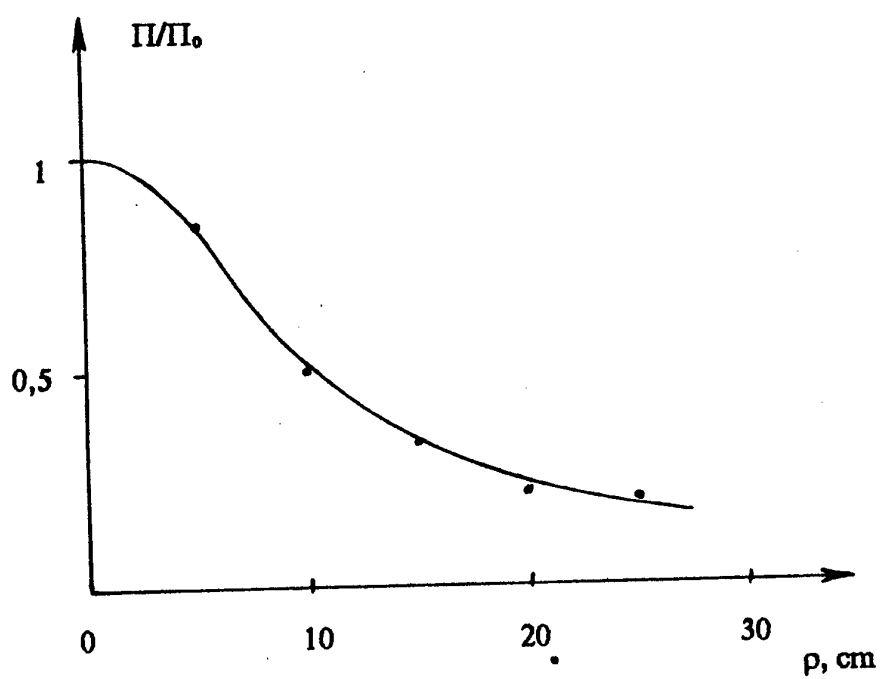
Fig.6. Radial distribution of relative field intensity in the MW beam

A metal mirror ($\varnothing$ 600 mm) can be installed in the chamber on a distance of 1 m from the lens. The mirror focuses the MW radiation on an axis of the chamber illuminators (see Fig.1). On Fig.7 and 8 the measured configuration of an electric field at linear polarization in the zone of beam focus is shown. The x axis is parallel to the magnetic component of the electromagnetic field. The z axis is parallel to the electric component. The y axis is parallel to the direction of the electromagnetic energy flow. Near the focus the electric field distribution can be approximated by the Gauss law with characteristic sizes $x_0 = 2,5$ cm and $z_0 = 5,2$ cm. Maximal electric field in the focus $E_0 = 7 \cdot 10^3$ V/cm. The described below experiments were carried out just with presence of the focusing mirror and with the linear polarization of a field.

The installation is equipped with a set of diagnostic devices for measuring the following parameters: the microwave field amplitude and polarization; a time-integrated and a high speed camera photo registration of plasma radiation at the discharge processes; spatial mean values of the plasma electron concentration n_e; registration of gas dynamical perturbations by the shadow method; parameters of gas dynamical waves from the discharge area; spatial mean gas temperature of the discharge region.

2.2 Installation II

Besides the described installation, another one is prepared for experiments in the MSU on physics department [4-6].

The generator (pulsed magnetron) can operate either in a single pulse mode, or in a mode of repeated pulses. It has the following characteristics: wave length $\lambda = 2.4$ cm; MW pulsed power W < 600 kW; a pulse duration 5 - 200 μs; pulse period-to-pulse duration ratio is 1000. A specially developed pulsed modulator with a partial discharge of a store capacitor is used for the magnetron power
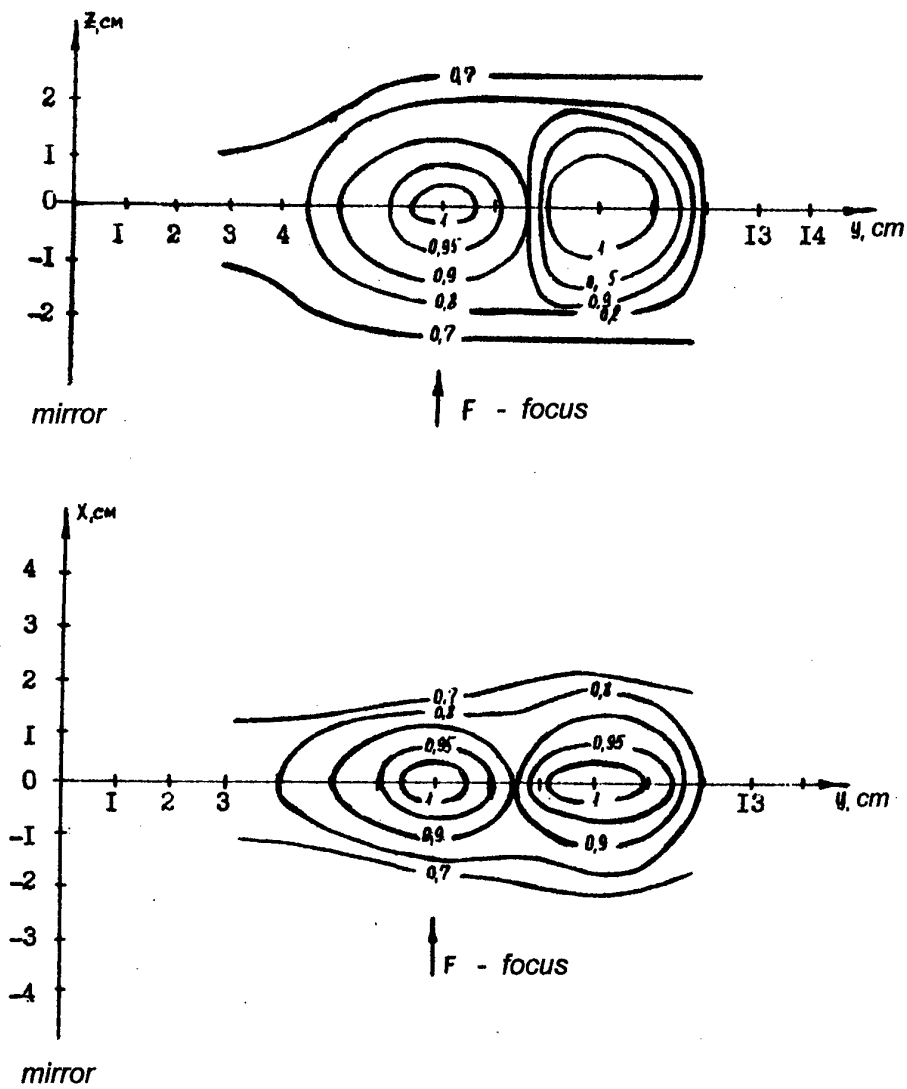
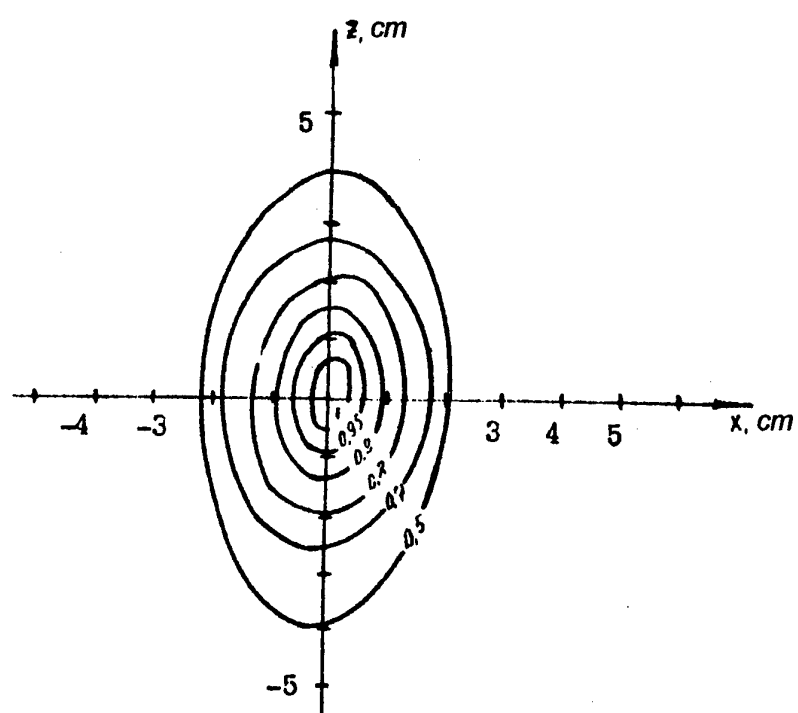Fig.7. Distribution of relative field intensity E/Eo near the focal point F

in zy and zx planes

Fig.8. Distribution of relative field intensity E/Eo in a plane zx,

which contains the focus

supply. The operation of a pulsed modulator is based on energy accumulation during time between pulses and powerful output during a pulse. The microwaves energy propagates from the magnetron to a discharge chamber along a rectangular 9,5 x19 mm waveguide. The whole waveguide is air-tight and is filled by SF_6 up to the excess pressure of 6 atm.

The microwave energy enters a cylindrical vacuum chamber through a conical diffuser with a polysterene lens ($\varnothing$ 600 mm, focus 80 cm). The vacuum system makes it possible to provide discharge experiments at initial pressure from 10 to 760 Torr. The focusing lens is a vacuum-tight separator between the chamber and the waveguide.

The vacuum chamber consists of two sections. A larger chamber section chamber ($\varnothing$105 cm, 300 cm length) is mounted on a trolley, it can be connected with a smaller chamber section by a special lock, that provides an access inside the chamber. Running wave mode is provided by microwave absorbing cover of the chamber wall opposite to the lens.

To control the discharge plasma parameters, the installation can automatically generate either two-stage pulses of one MW source, or sinchronised series of pulses originating from two sources. E.g., as it has been shown in experiments, rectangular microwave powerful durable pulses do not result in effective energy input into the focal region, which prevents, e.g., effective gas heating and combustion ignition. In order to provide the discharge localization in a previously specified region, instead of a running MW discharge mode, a new method of programmed effect can be applied. To implement it, the breakdown is produced by a powerful radiation pulse, which is short enough to provide absense of the energy absorption region movement. The second, long MW pulse is weak to cause breakdown and plasma movement, but it can support the previously formed plasma.

The experimental installation is supplied by a complex of diagnostic equipment. It comprises spectrographs and monochromators, used for absolute and relative intensities registration of spectral lines, molecular bands, and continuous spectrum. Both standard and specially developed methods for diagnostics of the free located microwave discharge are used, they provide measurement of electrical field intensity in plasma, electron energy distribution function, density and temperature of electrons, vibrational and gas temperature. Schlieren laser snapshot photographs of the discharge area are taken during a sounding laser or a flashlamp pulse. A synchronization system can change breakdown - flash time delay from 0 up to 1 s. To measure the electron density at pressure higher than 10 Torr, a standard method of plasma sounding by microwave radiation (wavelengths from 4 up to 8 mm) is used.

2.3 Methods of Spectral Diagnostics

For measurement of parameters of plasma and gas of an investigated microwave discharge there has been used a diagnostic set up containing a spectrorgraph STE-1 and a monochromator DFS-12. The monochromator has a constant dispersion 0.5 nm/mm in working area of a spectrum from 300 up to 650 nm. The spectrorgraph dispersion changed from 0.3 up to 1.2 nm/mm with change of a wavelength of registered radiation from 200 up to 1000 nm. These spectral devices make it possible to record spectral lines broadening and to resolve rotational structure of molecular bands [4].

Gas temperature and elecron concentration have been determined from plasma radiation spectra on base of the following. A radiation intensity corresponding to a transition between rotational levels of the electronic-vibrational excited states can be expressed as:

$$I_{\to''} = n_{p'v'j'} \, A_{\to''} \, h\nu_{\to''} \, \Delta\Omega/4\pi,$$

in which $n_{p'v'j'}$ is the population of an electronically excited state p′, with vibrational quantum number v′, and rotational quantum number j′, $\nu_{\to''}$ and $A_{\to''}$ are the wavenumber and the transition probability for the given spectral line, $\Delta\Omega$ is the solid angle of observation and h is Planck's constant. In the adiabatic approximation, the corresponding transition probability $A_{\to''}$ is a product of electronic, vibrational and rotational fractions and can be expressed as:

$$A_{\to''} = (64\pi\nu^3/3h) \, A_{p',\,p''} \, q_{v',v''} \, S_{j',j''},$$

where $q_{v',v''}$ is the Frank-Condon factor.

In the case that the rotational distribution of the upper state of a molecular radiative transition is a Boltzmann distribution, the intensities of the rotational lines $I_{\to''}$ are directly linked to the rotational temperature through:

$$\ln(I_{\to''}/\nu^4_{\to''} \, S_{j',j''}) = -\,hc\,F(j')/(kT^*_{rot}) + const,$$

in which F(j′) is the energy of the upper level in cm^{-1}, k is Boltzmann's constant and c is the velocity of light. The plot of the $\ln(I_{\to''}/\nu^4_{\to''} \, S_{j',j''})$ versus the rotational term values F(j′) gives a so-called Boltsmann plot. The rotational temperature can be obtained from the slope of this plot. Due to the fact, that the rotational constants of the ground state B^o and excited state B′ are different (the difference is especially large for the hydrogen molecule and the difference is very small for the nitrogen molecule) the rotational temperature of the ground state T$^o_{rot}$ and the rotational temperature of the excited state T$^*_{rot}$ will in general be different. From

the last equation and the expression for the rotational term it is easy to obtain a relation between the two temperatures with good accuracy:

$$T^{o}_{rot}/\ T^{*}_{rot} = B^{o}/B'.$$

Microwave discharge is spatially non-uniform if pressure of gas (nitrogen, air, hydrogen, helium, argon) exceeds 200 Torr. The plasmoid is a set of thin channels with diameters being about 0,1-0,3 mm. They are stretched along a vector of the microwave electrical field. In this work the concentration of electrons in the channel of initiated microwave discharge was determined from Stark broadening of a spectral line H_{β} with $\lambda = 486,1$ nm. At high electron concentration $(n_{e} > 10^{14}$ cm$^{-3})$ the Stark broadening of hydrogen lines is the most effective mechanism of line broadening.

3. The Initiated Subcritical Streamer Microwave Discharge in a Wave Beam

For general information about the object under investigation, a typical time integrated photo frame of the initiated subcritical streamer discharge in a microwave beam is shown on Fig.9; air pressure p = 330 Torr, τ= 40 μs, E_{0} = 5,7kV/cm (here "time integrated" is understood as having exposition time exceeding τ). The last value is approximately 2,5 times less than the critical field level E_{cr}. (For air $E_{cr} = 40p$ [V/cm], here p is expressed in Torr.) The discharge is initiated by a leaden ball placed in the MW beam focus..

The initiating ball having a diameter 2a = 2,5 mm can be seen on the frame (at its center). This size can serve as a scale of the image. The focusing mirror is on the right, i.e. the vector of MW power flow Π_{0} is directed to the left, and $\mathbf{E_{0}}$
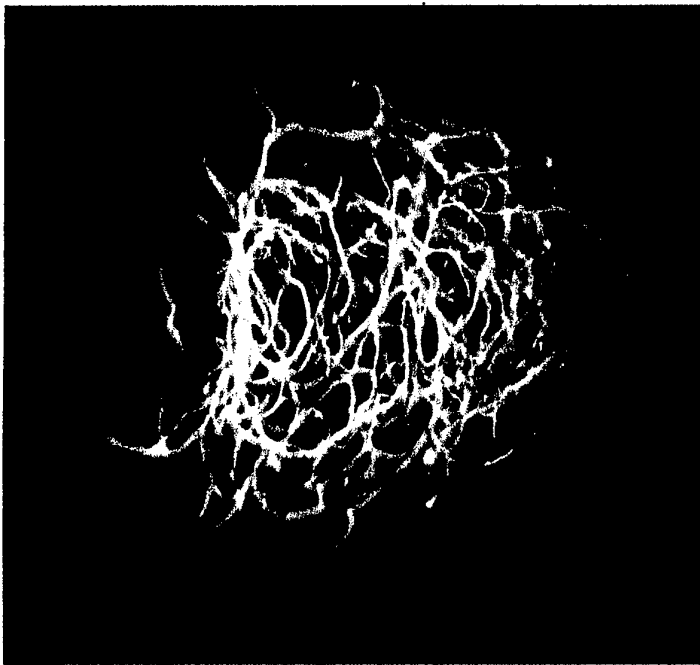
Fig.9. A ball-initiated streamer MW discharge with a developed structure

(p = 330 Torr, τ = 40 μs, E_0 = 5,7 kV/cm, 2a = 2,5 cm)

lays in the plane of the figure normally to Π_0. (In all the figures given below this position of Π_0 and E_0 is kept, as well as the ball's material and size).

One can see that the discharge is a chaotic structure of plasma channels. Their characteristic diameter is about a fraction of mm, and a characteristic distance between the channels is a fraction of λ. Such a form of the discharge (one can call it a streamer discharge with developed structure) under such experimental conditions is observed only at rather high gas pressure and duration time (with p>500 Torr and $\tau > 10^1$ μs). At shorter τ and lower E_0 the structure of the discharge simply has no time to develop.

Basic qualitative and some quantitative properties of such discharges are presented below.

4. Microwave Breakdown

At realization of the subcritical discharge, the problem of ignition is the first to arise. The discharge needs to be initiated. One of possible ways of initiation is to concentrate the electric field by insertion of metal bodies (for example, a ball or a so called vibrator – a thin needle parallel to E_0) into the EM beam. In this case on their poles, where E_0 is normal to metal surfaces, there is a local field amplification, and its value can exceed the critical breakdown level. E.g., the field is tripled on a ball surface if its diameter 2a is much less than λ, still more amplification takes place in case of vibrator. On Fig.10 a photo frame of the discharge is given at p = 760 Torr, E_0 = 3 kV/cm and τ = 40 μs. The discharge is initiated by an aluminium vibrator with length 2l = 10 mm and the diameter 2a = 0,8 mm. On the figure the vibrator is located at the left side. The distance between its radiating ends can serve as a scale of the image. E_0 is about 10 times less than the corresponding E_{cr}, i.e. subcriticality $\Psi = E_{cr} / E_0$ =10. One can see that even at
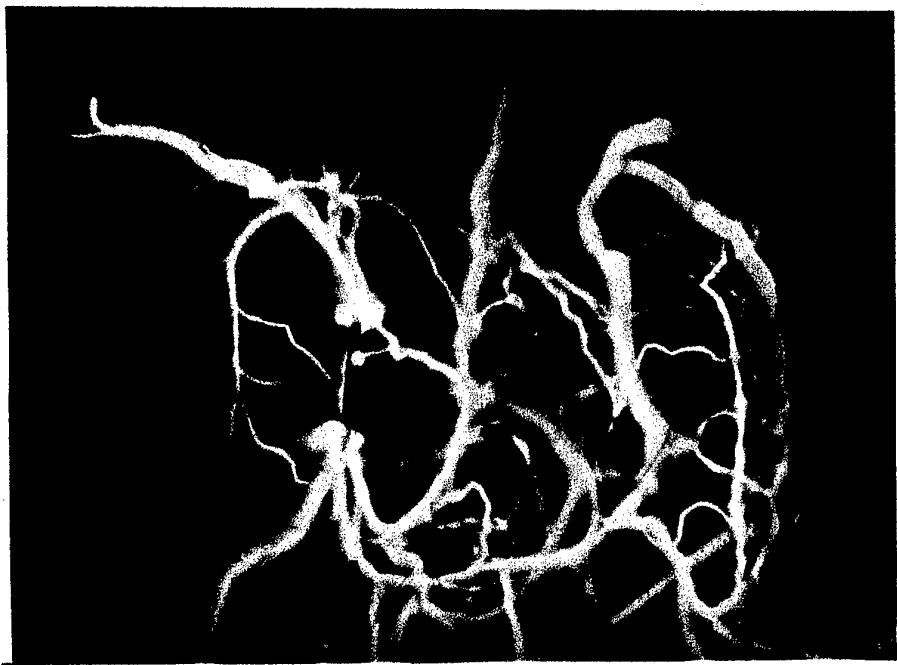
Fig.10. A streamer MW discharge initiated by a metal vibrator

(p = 760 Torr, 2l = 10 mm, 2a = 0,8 mm, E_o = 3 kV/cm)

such a high subcriticality the discharge had a well developed streamer structure at the pulse end.

A series of similar experiments with with the same E_o = 3 kV/cm and 2a = 0,8 mm, in which the vibrator length 2l was varied only, has shown that the size 2l = 10мм is a minimal one which provides the atmospheric air breakdown and the discharge inizialisation.

For prediction of breakdown under conditions of specific scientific or technical application one can use results of work [7]. It yields the following expression for the amplitude of electric field on poles of the vibrator:

$$E_n \cong E_o \sqrt{\{1 + A[(1/kl)\cdot\cos kl) + \sin kl)]^2 + \{A[(1/kl)\cdot\sin kl) - \cos kl)]^2}, \quad (1)$$

$$A = [2/(3\pi)]\cdot(z_0/z)\cdot(h_\partial/a),$$

here $z_0 = 120\pi$ Om is the wave resistance of vacuum, $h_\partial \cong (4/\pi)\cdot l$ - working length of the vibrator, $z = \sqrt{R_\Sigma^2 + X_0^2}$ - module of its complex resistance, ,

$R_\Sigma \cong (1/6)\cdot(z_0/\pi)\cdot(kh_\partial)^2$ - resistance of radiation of the vibrator,

$X_0 = -(z_0/\pi)\cdot[\ln(l/a) - 1]\cdot ctg(kl)$ - its reactive resistance at l/a>> 1 and

$X_0 = -(z_0/\pi)\cdot[(h_\partial/(3ka^2)]$ - its capacitor resistance with l = a and k = 2π/λ..

The discharge ignition has a necessary condition $E_{br} \geq E_{cr}$. Let's check up whether this condition is met for the experiments corresponding to Fig.10. From (1) it follows that for these experiments E_{br}/E_o = 9, i.e. the concentrated field E_{br} = 27 kV/cm, that agrees with the breakdown threshold value (E_{cr} = 30 kV/cm at p = 760 Torr) within the limits of experimental accuracy.

So in each particular case with given p and E_o, it is possible to choose the sizes of the initiating vibrator, which provide that the breakdown necessary condition $E_{br} \geq E_{cr}$ is fulfilled, on base of estimates (1). It does not guarantee however that breakdown will always take place. It follows from (1) that the field amplification factor A is in inverse proportion to a. However, it does not mean,

that by reduction of a one can achieve breakdown in a gas with a certain p even at very small E_0. The region where the necessary field enhancement takes place has a characteristic length which is approximately proportional to a, this region vanishes at considerable reduction of a, and electron diffusion from this region becomes essential, that should be taken into account (see [8]). And at last, it is necessary to pay attention, that at very large subcriticality the type of the discharge can change. In this case, as it will be shown below, the discharge cannot have the developed streamer structure.

5. The Microwave Discharge Physics

Experiments at different p and τ were carried out in order to study the processes of the discharge development. E_0, as a rule, was close to the breakdown threshold, that made it possible to prolong these processes . The experiments have shown, that at the longest possible τ the discharge has the developed structure only at $\Psi \leq 20$. We shall consider only the discharges with the developed structure.

5.1. Diffuse Stage

The experiments show, that the initiated discharge begins to develop on poles of the initiator in areas, where the electric field E exceeds E_{cr}. The discharge starts in a form of diffuse formations growing along $\vec{E}_0$.

On Fig.11 the discharge photo frame is presented for a case of p = 20 Torr, E_0 = 0,8 kV/cm, and τ < 2 μs. One can see that during this time two 1 cm long plasma columns have grown from the poles of the sphere. Thus, their growth speed was about 10^6 cm/s.

Low pressure was deliberately chosen at this experiment. The lower is p, the longer is this stage, and the easier is it to study it. With growth of p the initial

diffuse plasma distribution forms a background, inside which more complicated structures grow up, duration of this stage and volume of the discharge are reduced radically. It is difficult to demonstrate this stage in experiments at high pressure.

The diffuse MW discharge is a process ruled by field concentration and ionization. During this stage a strong coupling of plasma formation and field redistribution takes place.

The change of electronic concentration n_e in the elementary case can be described by the equation of electronic balance with processes of ionization, attachment, and diffusion. It is possible to assume, that the frequency of ionization depends only on the field. Computation of the MW field should be based on the Maxwell equations with the "delay".

In fields which are of the same order of magnitude with E_κ, the frequency of ionization is possible to be taken as

$$v_i = v_a (E/E_k)^{5,3}, \qquad (2)$$

here $v_a = 2 \cdot 10$ p, 1/s is the frequency of attachment with dissociation, and E is the field in plasma. In such a simple approach it is (2) that sets a connection between n_e and E. At the diffuse stage only E is changing at plasma formation. Gas heating is negligible, and one can consider E_{cr} and v_a to be constants in (2).

The analysis of the equations shows, that in a course of the diffuse stage the field E practically does not vary in plasma and on its borders parallel to $\vec{E}_0$, and is very close to E_0. At the plasma borders which are normal to $\vec{E}_0$ the field grows in comparison with its initial value. It results in growth of plasma columns along $\vec{E}_0$ (see Fig.11).

The speed of the diffuse border movement can be estimated as

$$V_\partial = 2\sqrt{D_a \cdot (v_i - v_a)}, \qquad (3)$$
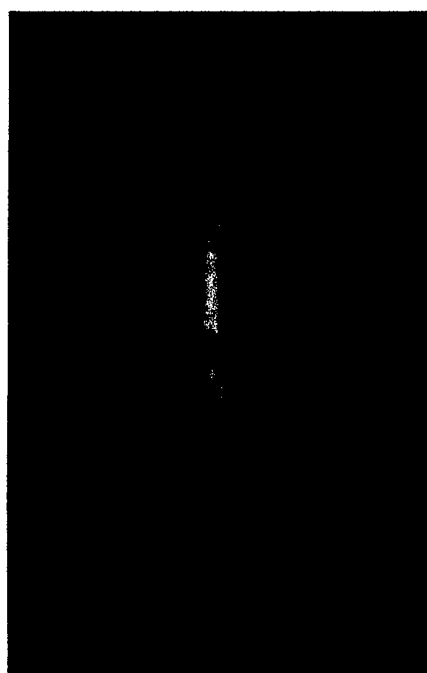
Fig.11. Diffuse stage of an initiated MW discharge
(p = 20 Torr, E_o = 0,8 kV/cm, τ < 2 μs, 2a = 2,5 mm)

Here at $E \cong E_{cr}$ the coefficient - $D_a = 1{,}4 \cdot 10^4/p$, cm^2/s. There is a difficulty here. In (3) v_i is essentially dependent on E, see (2), which in turn depends on distribution of n_e which is previously unknown.

The relation E/E_{cr}, according to the formulae (2) and (3), is approximately equal to 2 for the discharge conditions corresponding to Fig.11 (i.e. at $V_D \cong 10^6 cm/s$).

5.2. A Stage of Ionization and Heating

As it was mentioned above, with increase of p the structure of the discharge becomes complicated. For example, on Fig.12 a photo frame of the discharge at $p = 45$ Torr, $E_o = 1{,}5$ kV/cm and $\tau = 17$ μs is presented. One can see that inside the initial diffuse plasma formations there appear thinner and brighter plasma channels. Their diameter is approximately equal to 0,5 mm. Channels are extended in the direction of $\vec{E}_o$.

Note that contrary to the case of Fig. 11, there appear bright "caps" near the poles of the initiating sphere. The analysis of experimental results shows, that they occur only with presence of bright channels and are connected to evaporation of a material of the sphere (here it is lead). Thus, gas temperature on its surface should be not less, than the temperature of evaporation (here $2 \cdot 10^3$ K).

The physics of the channels formation determined by processes of ionization and heating in the initially diffuse plasma. An analysis of these processes can be made on base of equations of field, ionization, and isobaric gas heating. As the channels are long and thin, one can consider the field there to be constant at growth of n_e. Then in equation (2) only v_a and E_κ are varying, as the gas density N falls (due to isobaric local heating in the channels).
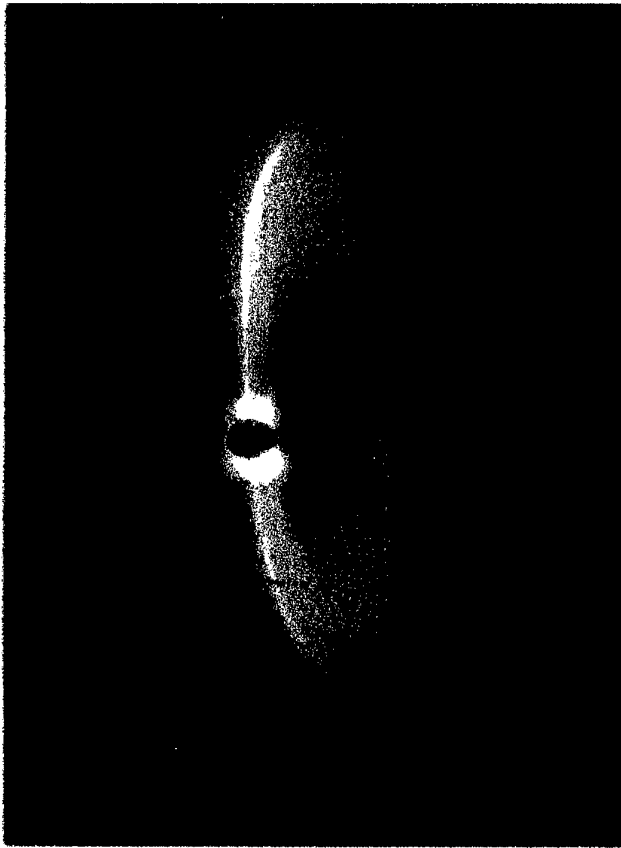
Fig.12. A diffuse initiated MW discharge with ionization and heating in channels

(p = 45 Torr; E_0 = 1,5 kV/cm; τ = 17 μs; 2a = 2,5 mm)

At experimental conditions with a limited t" and p < 50 Torr this stage is the last stage of the discharge development. At higher p the structure of the discharge again becomes still more complicated.

5.3. A Streamer Stage

At high pressure (p > 50 Torr) the channels begin to elongate. Their ends approach to borders of the initial diffuse area, and streamers begin to grow from these places. Here by the term "streamer" we mean a plasma filament which is growing due to concentration of field near its tip. That is why streamers can grow to areas where an initial field level E_o is much less than E_{cr}.

Fig.13 shows a photo of a discharge at p = 75 Torr, E_o = 2 kV/cm, and τ = 36 µs. One can see that this discharge looks like a of system of plasma streamers which are bending and branching. Cross section of a channel contains a bright channel surrounded by a diffuse environment.

As p grows, this diffuse environment becomes less expressed, but still exists: see, for example, Fig. 9, Fig. 10, Fig. 14.

From the qualitative point of view the physics of streamers' growth is quite clear. As p grows, the characteristic diameter of the channels decreases, and the degree of field concentration grows. According to (2), it results in activating of ionization process at the tips of the channels, and in their lengthening. As the tip approaches to the border of the diffuse area, there begins a local growth of n_e with formation of a spherical diffuse plasma lobe. The channel grows into it, and etc.

Thus, there is always a diffuse precursor before a streamer. At the same time, the streamer's head diameter defines the channel. The presence of the internal channel distinguishes streamers from of an electronic avalanche which frontal part is broadening at propagation (see, for example, fig.11).

Fig.13. A streamer initiated MW discharge

(p = 75 Torr; E_o = 2 kV/cm; τ = 36 μs; 2a = 2,5 mm)
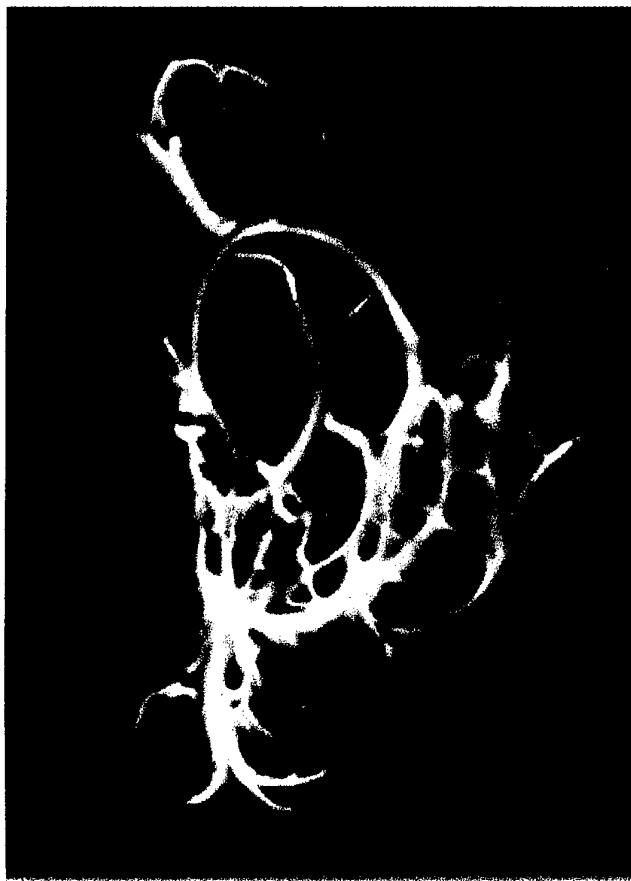
Fig.14. A streamer initiated MW discharge

(p = 120 Torr; E_o = 2,5 kV/cm; τ = 36 μs; 2a = 2,5 mm)

A field in area of streamer head is essentially higher than E_0. It is determined by its total configuration and, naturally, does not coincide with the direction $\vec{E_0}$, and some parts of streamers can be even perpendicular to $\vec{E_0}$ (see Fig.13,14).

The photos show that streamers grow primarily towards and across $\vec{\Pi_0}$, that results in a movement of the discharge front towards a MW radiation source.

Experiments with variation of p, E_0 and τ [9] yield the following approximation of an average speed of movement of front of the subcritical streamer discharge:

$$V_f = (1/\sqrt{p}) \cdot (3 \cdot 10^4 \sqrt{p} + 1{,}7 \cdot 10^{-2} E_0 \cdot p \cdot \lambda); \text{ cm/s,} \qquad (4)$$

here E_0 is expressed in V/cm, and λ is in cm. One can conclude that at p>100 Torr V_f is about 10^5 cm/s. The first factor in (4) takes into account stochastic variations in a direction of growth of a streamer. The second factor is essentially an average rate of growth, it is about 10^6 cm/s at p>100 Torr.

5.4. Resonant Stage

The discharge we consider in this work is a streamer discharge in MW radiation, it has differences from streamer discharges in a steady electric field. Its parts with sizes about $\lambda/2$ can have resonant properties. It has been confirmed by our experiments.

Fig.15 shows a fragment of high speed photo frame of the discharge which time-integrated photo is given on Fig.9. The fragment corresponds to exposition time of 1,5 μs and a moment of time 10 μs after the breakdown. The initiating ball is situated approximately at the center of the image, about 10 cm to the left of luminous channels located on the discharge front (it is found out from the time-integrated photo). Neither the ball, nor streamers situated between it and the front
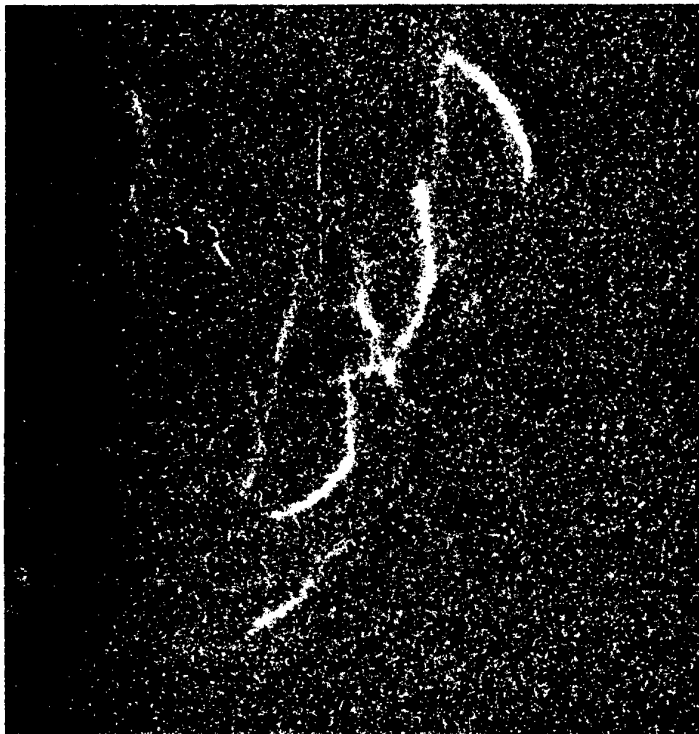
Fig.15. A photo frame of a streamer MW discharge with a developed structure
(time of exposition is 1.5 μs; 10 μs from the moment of breakdown; p = 330 Torr;
E_o = 5.7 kV/cm)

not shine and, naturally, are not visible. The luminous streamers are about $\lambda/2$ long, they are approximately parallel to $\vec{E}_0$. Their length can serve as a scale of the image. Their diameters are about 1 mm.

In order to examine energy balances of the resonant parts of the streamers, one can consider them as resonant MW vibrators. For our experimental conditions their characteristic length h_{eff} is 3 cm, effective voltage amplitude is U = 17 kW. In [10] a resistance of such plasma vibrator is estimated as R_Σ = 100 Ω. The corresponding estimate for an amplitude of current is I $\cong$ 80 A, and power $\Delta P >$ 100 kW. Such an intensive power absorption is accomplished with formation of shock waves, which is confirmed by our experiments. Actually, at such discharges one can hear a loud sound pop.

A characteristic shadow photo frame of a discharge at p = 200 Torr is shown on Fig.16. One can see a shock wave generated by the discharge as a whole (on the right). Inside the discharge area there are observed practically cylindrical shock waves, which are generated by the resonant parts of streamers. The quantitative processing of a series of similar photos shows, that practically all the MW energy is absorbed in these parts of streamers on the discharge front [11].

A frame-by frame analysis of high-speed photo registration of the discharge shows, that the characteristic time of energy absorption in the resonant parts of streamers is about 1 microsecond. For example, Fig.17 shows three sequent photo frames of the discharge for the conditions of Fig.9, with time period being 1.9 μs and exposition being 1.5 μs. On the second frame one can see a flare of a first resonant vibrator. On the first frame it is not seen yet, and on the third frame it does not shine any more. (By the way, on the third frame there are seen three new separate resonant vibrators). If one takes $\Delta t = 10^{-6}$ s, as it follows from the analysis of Fig.18, then energy input into the vibrator exceeds 0.1 J (at the

Fig.16. A shadow photo frame of an initiated streamer MW discharge
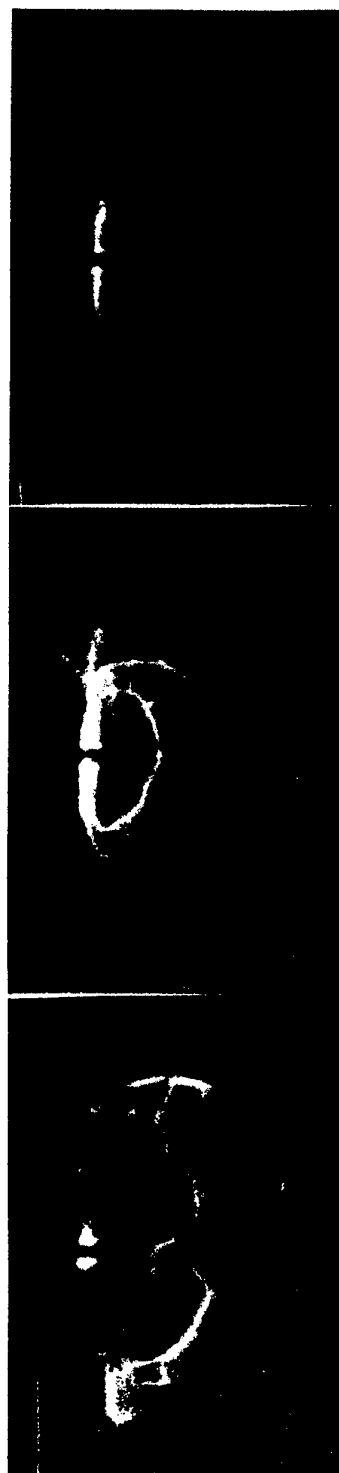
(p = 200 Torr; E_o = 3 kV/cm)

Fig.17. High speed camera frames of a start period of development of an initiated
streamer MW discharge (time of exposition is 1.5 μs; period of time between
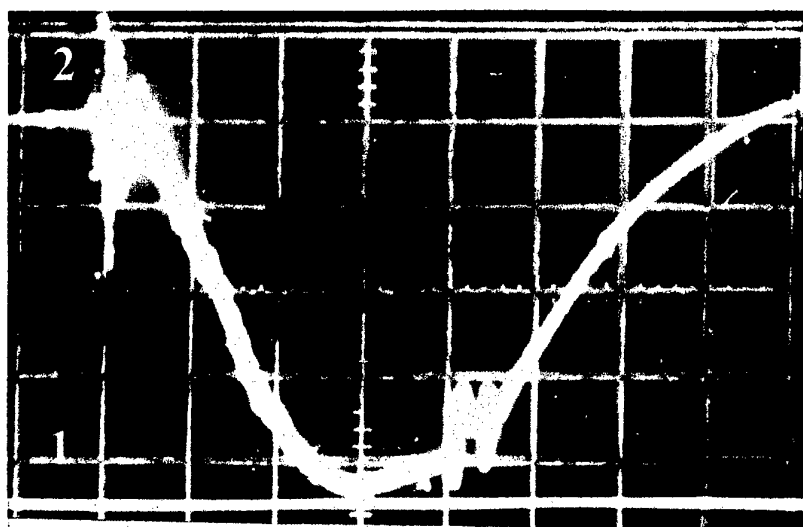the frames is 1.9 μs; p = 330 Torr; E_o = 5.7 kV/cm; 2a = 2.5 cm)

Fig.18. An oscillogram of a $\lambda = 1$ signal beam which passes through the discharge plasma (p = 120 Torr; E_o = 4.8 kV/cm; $\tau = 40$ µs)

previously estimated value of ΔP). These estimations show that it will result in gas heating to some thousands degrees.

5.5. Plasma Decay Stage

It is natural, that behind the discharge front and after termination of MW pulse the plasma decay process begins. Its analysis can provide us with an additional information on properties of the discharge. With this purpose a temporary dependence of average electronic concentration $\bar{n}_e$ was measured.

To implement it, the discharge area was sounded by a continuous microwave radiation with $\lambda = 1$ cm. The signal attenuation due to interaction with plasma was measured. The axis of sounding was perpendicular to E - plane, it passed through an axis of a wave beam and was 2 cm shifted from a point of location of the initiator towards the radiation source. The cross section of the sounding beam was 3 cm.

The corresponding oscillogram for p = 120 Torr, E_0 = 4,8 kV/cm, and τ = 40μs is presented on Fig.18. Here the line 1 corresponds to a complete attenuation of the signal. An initial horizontal oscillogram part (the curve 2) shows a signal level at absence of plasma. Oscillations correspond to the MW pulse beginning and end moments.

One can see that at first the signal amplitude falls almost linearly, as the sounding beam is being blocked by the plasma. The rate of blocking corresponds to the speed of movement of the discharge front (which can be estimated as $\cong 10^5$ cm/s). The maximal signal attenuation is the same as an attenuation by a flat plasma layer with the same thickness as the plasma region size (as it is seen on the photo), and with plasma concentration $\bar{n}_e = 3,5 \cdot 10^{12}$ cm^{-3} (no reflection of MW is taken into account at these estimates).

The oscillogram shows that after 30 μs from the breakdown (when the discharge front passes through the sounding beam) the plasma begins to decay with a characteristic time being more than 100 μs. After the end of the MW pulse the rate of decay grows, but the characteristic time is still high (more than 10 μs). Such a long lifetime is characteristic to an equilibrium, thermal ionization in the streamers. The reduction of n_e in this case is connected with cooling of gas in the resonant parts of streamers due to heat conductivity.

Estimates on base of a dependence of a heat conductivity relaxation time, plasma region characteristic size, and heat transport properties of air yield the corresponding gas temperature about 10^4 K.

One should note, that in experiments at low p, when the diffuse discharge form takes place only, the oscillograms show that the decay of plasma practically followed the back front of the MW pulse, i.e. the characteristic time was less than 1 μs. The decay in this case takes place due to processes dissociative and three-particle attachment.

5.6. Sequence of Stages of the Streamer Discharge

To summarize the paragraph 5, let us consider a general description of development of the initiated streamer MW discharge from the moment of breakdown till formation of the developed structure.

Fig.19 a, b, c, d contains photo frames of the discharge at p = 300 Torr, $E_0 =$ 5 kV/cm and τ = 1, 3, 7 and 36 μs. On the first frame one can see two streamers that grow along $\vec{E_0}$ from poles of a spherical igniter. Their length is 0.5 cm, hence, the average speed of their growth is not less than $5 \cdot 10^5$ cm/s. Each streamer has a thin (<0.5 mm) bright channel, and a diffuse envelope, which is also rather thin for
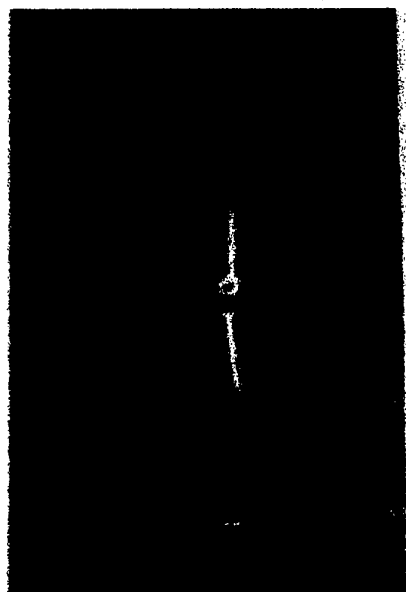
$\tau = 1 \ \mu s$

$\tau = 3 \ \mu s$

$\tau = 7 \ \mu s$

$\tau = 36 \ \mu s$

Fig.19.   Streamer microwave discharge in air

p=330 Torr, $E_{a0} = 5.7 \ kV/cm$

these conditions. One can also note a radiating edge of a hole in the upper side of the sphere, which is made for a thread that fixes the igniter.

From the second photo it follows, that at 3 μs after ignition a first resonant vibrator has already been generated, and the process of resonant energy absorption has already finished (the vibrator has "exploded"). It is stretched along $\vec{E_0}$, its length is about 3 cm, that practically coincides with a resonant length at given λ. As a result the gas in the vibrator has been heated up, and the streamer's luminous diameter in its central part has increased up to 1.5 mm. In this moment the process of evaporation of poles of the initiator is in progress already.

At the ends of a resonant vibrator the field is maximal. Under conditions of this experiment this field exceeds E_0. That is why the streamer is branching exactly in these places (see the second frame). In such a way a series of streamers is formed. The field configuration near the streamer is close to that of a dipole. The streamers grow along the field force lines, and they are shifted primarily in the direction towards the MW radiation source, as the initial MW beam is partially screened behind the paternal streamer. The field before this streamer is formed by an interference of the falling and the reflecting electromagnetic waves, it has a complicated but smooth azimuth distribution. Breakdown processes are known to be stochastic, it results in stochastic position of new streamers (e.g., the well known linear lightning has a complicated stochastic form). That is why a poor repetitiveness of the discharge spatial structure from pulse to pulse takes place.

The next frame (7 μs) shows a further growth of the streamers. They form a multimode electrodynamic system. In certain moments some of its parts can be characterized by resonant properties. These resonant parts are thickening and branching (see the third frame).

The last frame (36 μs) shows a complicated structure of the developed MW streamer discharge. However, each of its fragments can be analyzed in terms of the processes listed above.

The discharge length along $\vec{\Pi_0}$ at this moment is about 8 cm, which corresponds to $V_f \cong 2,5 \cdot 10^5$, that is in a satisfactory agreement with V_f calculated from (4) (pay account to stochastic features of the discharge, and to the influence of reflection on the field).

6. Characteristic Features of Streamer Microwave Discharges in Various Gases

The described processes of development of streamer microwave discharges are inherent to practically all the gases at a sufficiently high pressure. However, for different gases there are different specific features.

For example, a MW discharge in hexafluorated sulfur (SF_6) at p = 90 Torr, $E_0 = 5$ kV/cm, and $\tau = 10$ μs has a developed streamer structure (see Fig.20), but the "feather" channels are much longer than in air. It produces an impression of higher specific density of discharge channels in SF_6.

A MW discharge in hydrogen at p = 300 Torr, $E_0 = 5$ kV/cm, and $\tau = 10$ μs also has a developed streamer structure (see Fig.21), but there are practically no "feather" channels and fine structure, the discharge looks to be rarified.

And, at last, at discharges in helium at p = 300 Torr, $E_0 = 4.4$ kV/cm, and $\tau = 10$ μs, the diffuse regime takes place (Fig. 22). At p = 760 Torr, $E_0 = 5.5$ kV/cm, and $\tau = 10$ μs discharge in He has already the streamer structure, but the diffuse background is still well seen (see Fig.23).

Thus, the MW discharges in a focused of TEM EM beam in air, SF_6, H_2, and He are similar in the basic features (since physics of the separate stages described above does not depend on sort of gas). However, in air and SF_6 the diiffuse-streamer transition takes place at rather low p $\cong$ 100 Torr, while, say, in He the

Fig.20. An initiated streamer MW discharge in a hexafluorated sulfur

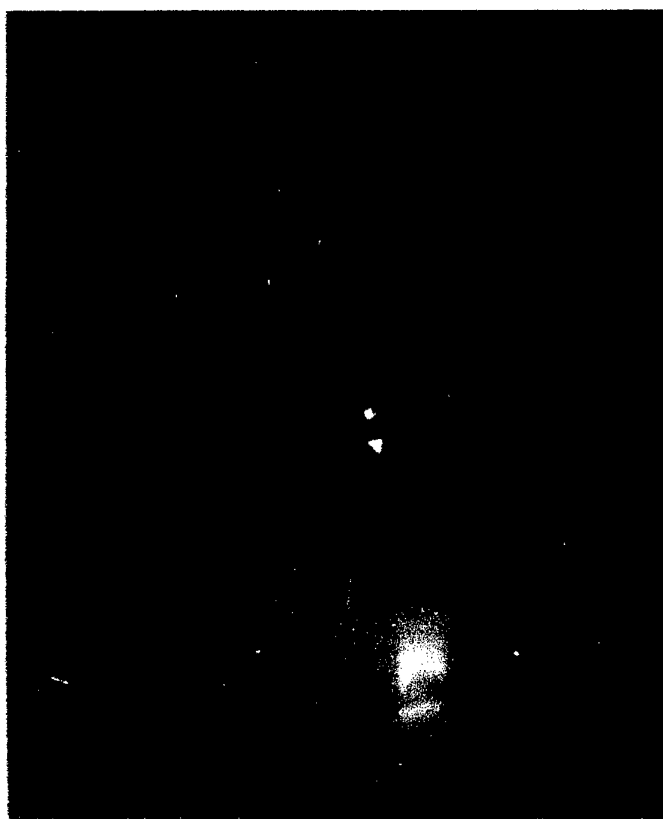(p = 90 Torr; E_o = 5 kV/cm; τ = 10 μs; 2a = 2.5 mm)

Fig.21.   An initiated streamer MW discharge in hydrogen

(p = 300 Torr; E_o = 3 kV/cm; τ = 10 μs; 2a = 2.5 mm)
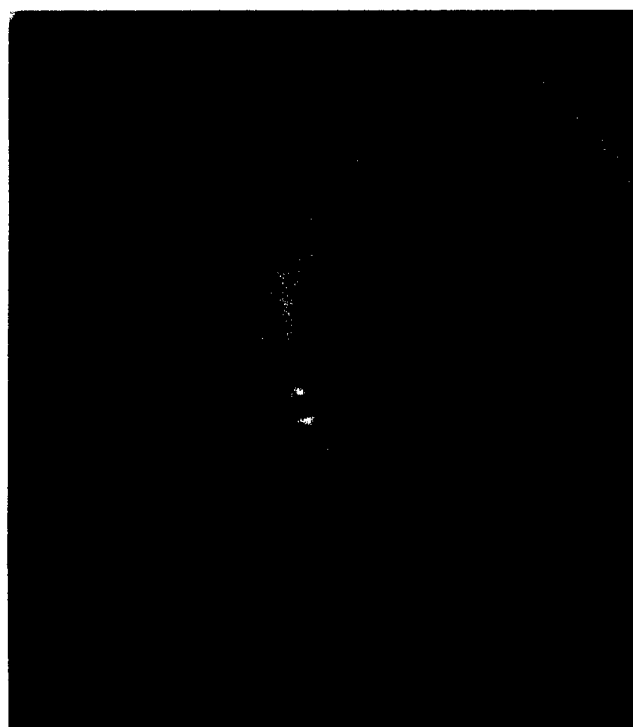
Fig.22.   A MW discharge in helium

(p = 300 Torr; E_0 = 4.4 kV/cm; τ = 10 μs; 2a = 2.5 mm)

Fig.23. An initiated streamer MW discharge in helium
(p = 760 Torr; E_o = 5.5 kV/cm; τ = 10 μs; 2a = 2.5 mm)

threshold pressure is much higher (p $\cong$ 500 Torr). Such distinctions take place because of different values of E_{cr}, v_a, D_a, v_i, etc.

It means that an additional study of discharges in combustible mixtures must be done before designing a MW system of fuel ignition in a supersonic flow.

7. The Microwave Discharge at High Subcriticality

From the practical point of view it is important to know, at what maximal subcriticality the streamer microwave discharge is carried out in the developed form.

As it was specified, it is possible to carry out a gas breakdown with a considerable subcriticality. Our experiments have shown, that subcriticality can be more than 100. At the same time, in this case the discharge essentially does not overstep the bounds of areas with an increased electric field E, which is formed by the initiator. For example, Fig.24 shows a microwave discharge in air at atmospheric pressure initiated by the a copper vibrator with 2l = 40 mm and 2a = 0,8 mm, at E_o = 600 /cm ($\Psi \cong$ 50) and τ = 40 μs.

In the photo frame one can see, that streamer channels depart from poles of the vibrator, and the discharge does not pass to the developed form. The material of surface at poles of the vibrator evaporates. Thus, in this case the temperature of the streamer channels exceeds 2 10^3 K.

Under conditions of our experiments the microwave discharges achieved the developed streamer form only at $\psi \leq 20$.

On base of our installation, without its modernization it was not possible to trace this transition in details. The installation in its present state is not intended for work with controllable small values of electric field E_o.
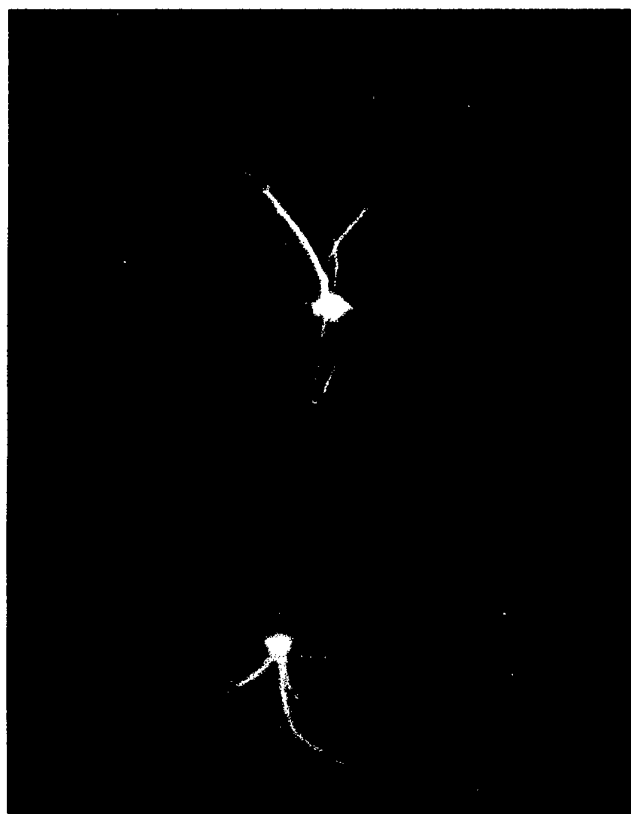
Fig.24. An initiated MW discharge at high subcriticality

(p = 760 Torr; E_o = 600 V/cm; τ = 40 μs; 2l = 40 mm; 2a = 2.5 mm)

8. Microwave Plasma Parameters

For MW plasma formation there has been used a pulsed (τ = 25 μs, f = 20Hz, W = 50-200 kW) microwave generator of 2,4 cm wavelengths. A 3 m^3 vacuum chamber was vacuumated (p ~ 10^{-2} Torr) and filled by either hydrogen, or a mixture of hydrogen with nitrogen up to 60-760 Torr. The measured values of electron concentration (meaned over time and channel diameter) is presented on Fig. 25. One can see that the electron concentration grows from ~10^{14} cm^{-3} at p = 60Torr to ~10^{15}cm^{-3} at atmospheric pressure. Experiments with time resolution have shown that the electron concentration is approximately constant during a 25 μs microwave pulse.

Gas temperature temporary dependence for a MW discharge in hydrogen is presented on Fig. 26. It is important that at an initial discharge stage the gas heating rate exceeds 300 K/μs. It is much higher than in pure air plasma at MW discharges at the same conditions [3].

Special experiments have been carried out in this work in order to check this result and to reveal a mechanism which results in such a fast heating of hydrogen. To obtain a sufficient accuracy of measurements, these experiments have been carried out under conditions of a pulse-periodic discharge in a $\varnothing$ 1×25 cm glass tube at pressure of hydrogen p = 0.6 Torr. The modulator produced 600 V, 200 μs pulses. Discharge current was 0.5 A. Electrical field in the discharge volume was measured with two probes. The electron concentration and temperature were determined from probe volt-current characteristics. Gas temperature was extracted from a rotational structure of the Fulcher α-spectrum bands. All parameters were measured with the temporary resolution.

At initial stage of the discharge a very fast gas heating is also observed (see Fig. 27). Estimates on base of the obtained experimental data have shown, that it
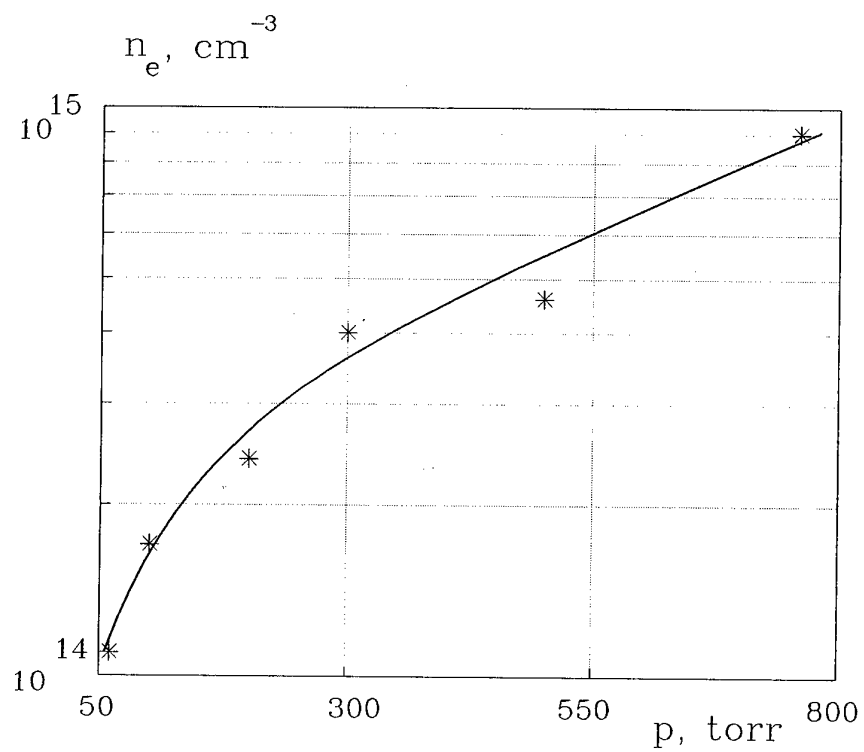
Fig.25. Pressure dependence of electron concentration in a channel microwave discharge in a hydrogen mixture
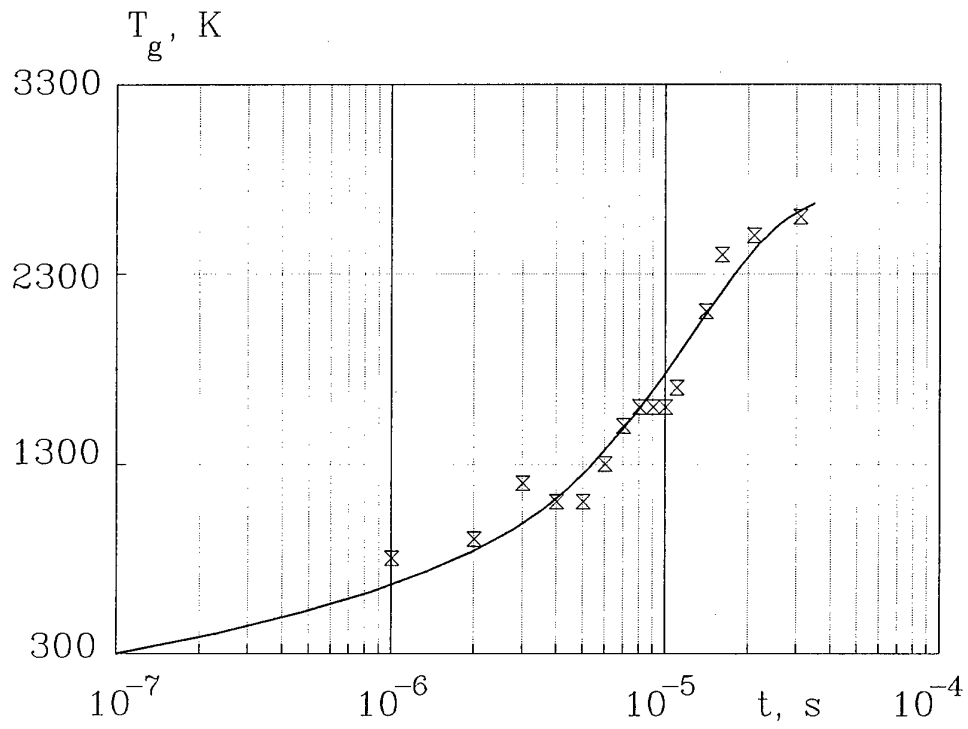
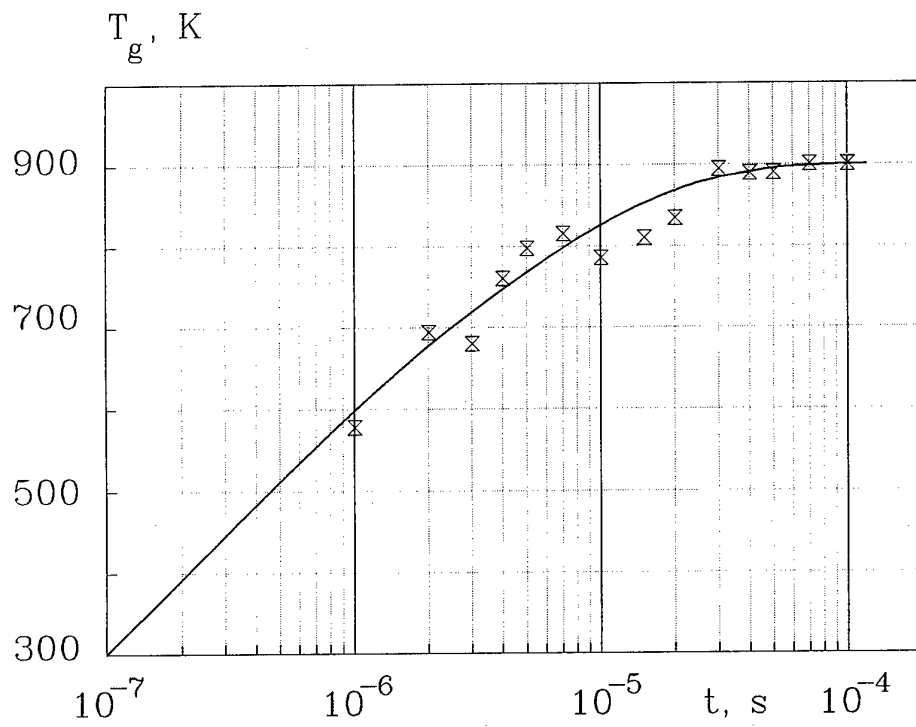Fig.26. Gas temperature versus time in a hydrogen microwave discharge plasma

Fig.27. Gas temperature versus time in hydrogen plasma at the tube discharge

cannot be connected with a usual mechanism of energy transfer from vibrationally-excited states to translational freedom degree of hydrogen molecules.

It results in a fact that simple extrapolation of results on MW discharges (see [3]) is incorrect, i.e. an additional extensive study is necessary to produce optimization for the discharge application for ramjet fuel ignition.

9. Numerical Simulation of the First Stages of Formation of the Subcritical Discharge

One of characteristic features of the MW discharge with the developed streamer structure is a lack of repetition of its form at different sequent pulses. Only the very beginning of the discharge repeats (to a certain extent), namely the stages from breakdown to formation of the first resonant plasma vibrator (see, e.g., the first frame on Fig.18). The process of formation of this vibrator can be simulated numerically.

The main spatial elements of the streamer microwave discharge which cause its unique character are the resonant streamer sections. Accordingly in the theoretical analysis of this discharge form the most attention was paid to the initial stage of its development. The prime questions to specify were the physics of processes leading to the growth of the streamer into the area with $E_0 \ll E_{cr}$, its transformation into resonant dissipative oscillator and so on.

9.1. Theoretical model

The streamer discharge in UHF electromagnetic fields is one of the finest and the most misunderstood nature phenomena. The phenomenon is very complicated and distinguished by diversity of types. Many experimental and theoretical investigations are devoted to study this phenomena. The attention to

the UHF discharges is caused by its advanced applications both technological and many others particularly in plasma aerodynamics of new generation aircrafts [11, 12]. In connection with these perspectives the gas discharge in UHF electromagnetic wave beams is especially interesting. The large experience is accumulated in the field of science both experimental and theoretical one. The wide series of study is executed with radiation wave length equaling 8.5 cm, 4cm, 2cm and 0.8cm[1-21]. This study is devoted to determination of the main physical mechanisms of discharge development in a gas with high and medium gas pressure.

In a dense gas an electrodeless UHF discharge arises in a beam of electromagnetic wave radiation. It have a complicated filamentary structure. The discharge is shaped as a net of very thin luminous filaments with bright fragments, which length approximatelly equals half wave length of radiation. The discharge consists of thin filaments selforganized into electrodynamic resonant vibrators and loops, rising one from another and propagating away from initiating point. The observations show that filament fragments of discharge net do not exist simultaniously but arise one from another. Each filament fragment at end stage of its evolution generates the cilindrical shock wave with initial Mach number equaling 1.5-2 [7]. It means that gas temperature in filaments is high. The 5-10 cm wave length radiation and 0.3-1 atm air pressure are good conditions for observation of the discharge [7, 8, 9]. It was discovered experimentally that after creation the arised discharge can be supported by radiation with electric field amplitude much less than critical value E_{cr}. It was shown that the electrodeless discharge can continiously exist even if undercritical parameter E/E_{cr} equals 1/50 and less [7]. It is possible by due to streamer effect and heating of filaments. The electric field on the ends of thin filament is much greater than unperturbed field. The discharge in the external electric field $E \ll E_{cr}$ was named the undercritical discharge.

There are many experimental studies of the UHF streamer discharges, but a satisfactory theory of this phenomenon is absent today. It is caused by very hard mathematical difficulties from one side and absence of clearness in physical mechanisms driving the process, from other side. The experiment s shows that the filament net consists of the interacting fragments with length equaling on the average 0.3-0.5 wave length. The average discription of discharge net is possible if we know the physics of a fragment. The mathematical model of a filament fragment of the undercritical UHF discharge and numerical investigations of its spatio-temporary evolution are presented herein.

It is well known that in overcritical UHF field ($E>E_{cr}$) free electron raises the ionization avalanche to create then spherical plasmoid. The plasmoid rises quickly along the electric field of radiation with the linear polarization. The cause of it is clear. If conductivity of plasmoid is high enough the polarization field at plasmoid poles is more than unperturbed external field and ionization at the poles is quicker than one at the equator [22, 23]. The initial spherical plasmoid transforms in ellipsoid and then in thin filament. The experiment show that when filament length reach the electrodynamical resonant value the ohmic heating cause the thermal explosion of that. The explosion shock wave is generated by the filament. Instead of filament with a high conductivity one has the filament with high temperature and low density. The life time of hot filament is controlled by usual thermal conductivity and can equal by order of value several tenth of second.

The undercritical discharge can't rise from one electron but need initial hot plasmoid with electrical conductivity. Each previous hot filament play role of initial element for next streamer filament. Thus the theoretic model of undercritical discharge should take into account not only the electrodynamics and physical-chemical processes (ionization, dissociation, electron dissotiative

attachment, molecular excitation et al) but also the filament ohmic heating by UHF currents.

It is clear that mathematical model of the streamer discharge in UHF electromagnetic wave should take in to account the 3D geometry, fully electromagnetic field discription selfconsistent with discharge, plasma chemistry and gas dynamics. So as investigation of filament net is very complicated the single filament fragment of the net is chosen as modelling object.

One found the method of calculation of the electromagnetic fields at thin filament with radius-length ratio up to minus several orders of value and with arbitrary conductivity distribution along filament by means of the integral Pocklington type equation [24, 25] for electric field amplitude $\mathbf{E}$ on the filament axis $\mathbf{z}$:

$$E(z) = E_{ext} + i \cdot \int_{-\infty}^{\infty} E(z') \cdot W(z',z) \cdot k \cdot dz',$$

where

$$W(z',z) = \frac{2\pi\sigma(z')}{\omega} \cdot \Psi(\sigma(z')) \cdot G'(z',z),$$

$$G'(z',z) = \frac{G(R)}{R^2} \times \left[(1 - i \cdot kR) \cdot \left(2 - 3\frac{a^2}{R^2} \right) + (ka)^2 \right],$$

$$G(R) = \exp(i \cdot kR) / R,$$

$$R(z',z) = \sqrt{a^2 + (z'-z)^2},$$

$$\Psi(\sigma) = \int_0^a J_0 \left[\cdot \sqrt{1 + i \cdot 4\pi\sigma/\omega} \cdot k^2 r dr \right],$$

$k = \omega/c$ - wave number, a - the filament radius, σ - conductivity, ω - field frequency, E_{ext} - external wave field. The integral equation has been solved numerically together with hydrodynamic equations in frame of isobaric approximation, which takes into account the next physical-chemical processes: 1) ionization in electric field by electron impact, 2) ionization in a hot gas, 3) electron dissotiative and 3-body attachment, 4) recombination, 5) electron diffusion with ambipolarity field and electron drift in UHF electric field taking

into account [20], 6) gas heating [11], 7) radiative losses. The our investigations show that it is not ecessary to include in the model the photoionization and preliminary ionization

$$\frac{d\sigma_n}{dt} = \left[K_i(E,N) - K_a(E,N) - R_{rec}(E,N) \cdot \sigma_n\right] \cdot \sigma_n \cdot N +$$

$$+ \frac{1}{N} \cdot \nabla \cdot \left(D(E,N,\sigma) \cdot \nabla(\sigma_n \cdot N)\right),$$

$$\frac{dT}{dt} = T \cdot \frac{[\sigma \cdot \Theta(\sigma) \cdot E^2 - Irad(p,T)]}{p \cdot C_p(p,T)},$$

$$\sigma = \sigma_n + \sigma_{Saha},$$

$$N = N(p,T),$$

$$p = Const$$

where

$K_i(E,N)$, $K_a(E,N)$- impact ionization and attachment velocity rates,

$R_{rec} = \alpha \cdot mK_{tr}/e^2$ (α- recombination coefficient),

σ_n - nonequelibrium conductivity,

σ_{Saha}- equilibrium conductivity,

$D(E,N,\sigma)$ - effective diffusion coefficient taking into account the ambipolarity and electron drift in UHF field [23],

C_p - air specific thermocapacity,

I_{rad} - radiation losses,

θ takes into account a skin effect,

p - gas pressure.

The model uses the experimental generalized data on electron temperature and mobility dependence on E/N and state equation for real air [26-31]. We use herein the isobaric approximation for simplicity. The latest calculations show that this approximation influence result insignificantly.

9.2.The simulation results

It is shown that only correct accounting of all the mentioned factors and their dependenses on electron and gas temperature gives possibility to simulate the evolution of the streamer discharge in UHF electromagnetic field, which is less than critical one. It should be noted especially the key role of free electron diffusion and oscillatory drift on the streamer ends [23] and gas heating. Fig.28-32 demonstrate the example of computer modelling of undercritical streamer discharge under conditions: p=0.25 atm, $E=0.25E_{cr}=2kV/cm$, a=0.07cm, λ=8.5 cm. Fig. 28-31 show surface and contour plots of the space-temporal distributions of UHF electric field amplitude $E(z,t)/E_{cr}$, gas density, $N(z,t)/N_0$ and $4\pi\sigma(z,t)/\omega$ on filament axis.

One can see the behavior of the undercritical streamer discharge. The initial hot plasmoid with small length and conductivity rises slowly until its length reach the resonant value. At that moment (τ = 13 μs) the streamer ends speed is maximum and equals $\sim3\cdot10^5$cm/s. After the resonance the streamer growth is stoped.

Fig.28, 31 and 32 show that streamer effect takes place indeed. The field increases on the ends of filament so as difference between ionization and attachment frequencies is positive inside the streamer. The electric UHF field distribution around the resonant streamer is shown on Fig.33. The field at the ends of streamer is much more than external field.

The conductivity in medium part of the filament at resonance moment is enough for the skin layer to be less than filament radius. It is the necessary condition for high enough quality of a resonant vibrator. But conductivity on the streamer head is relatively small, it is less than $\omega/4\pi$.
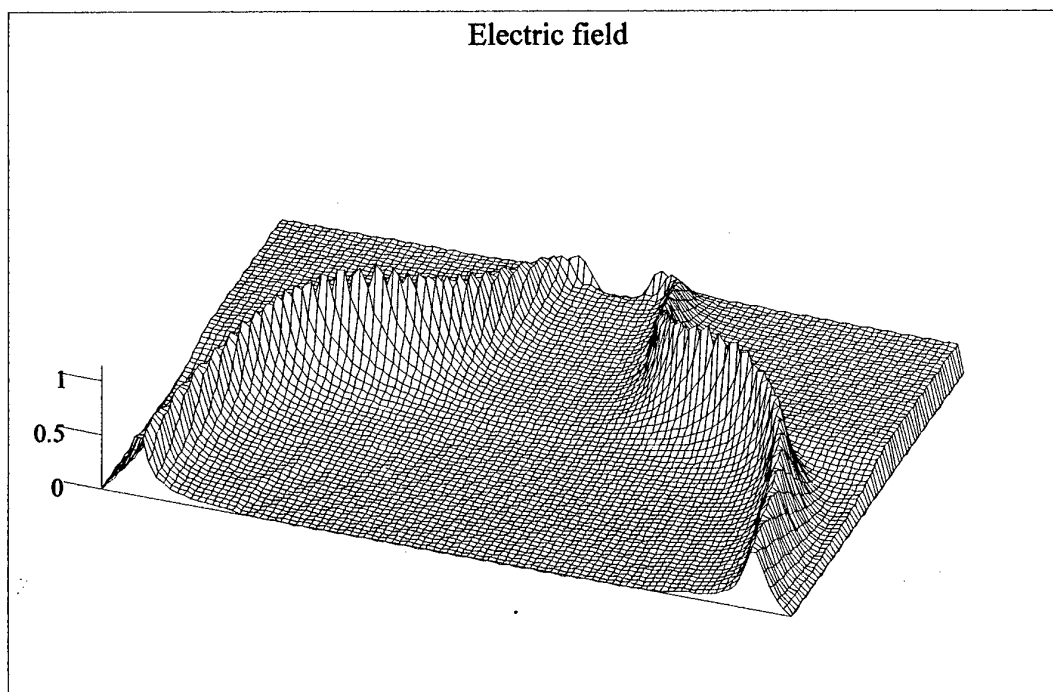
Electric field

ee

Fig.28. A surface plot of space-time distribution of a microwave

electric field amplitude $E(z,t)/E_{cr}$ on filament axis

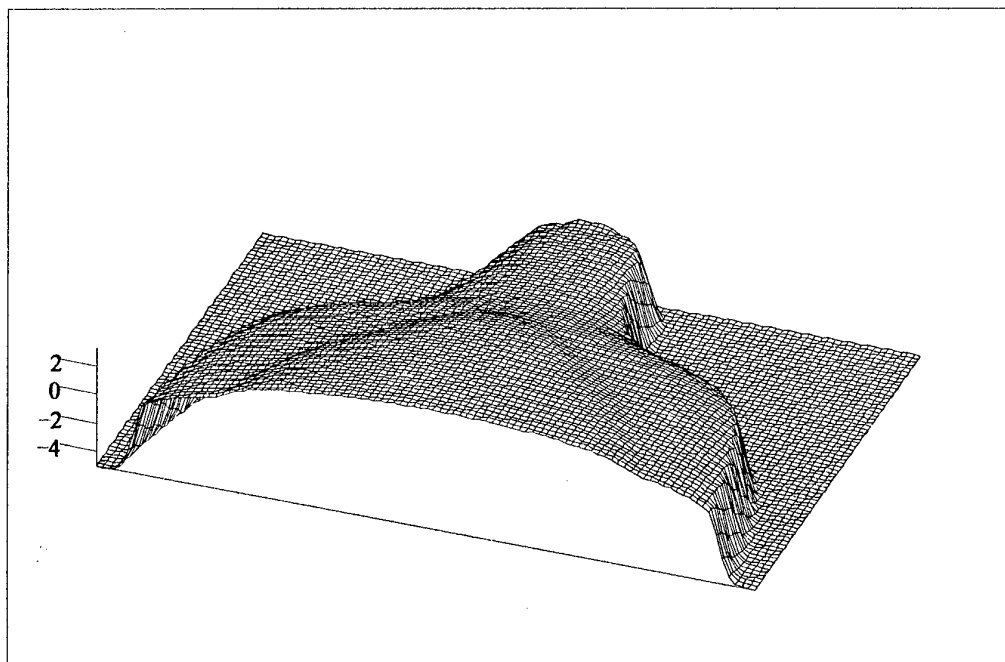(p=0.25 atm, E=0.25E_{cr}=2kV/cm, a=0.07 cm, λ=8.5 cm)
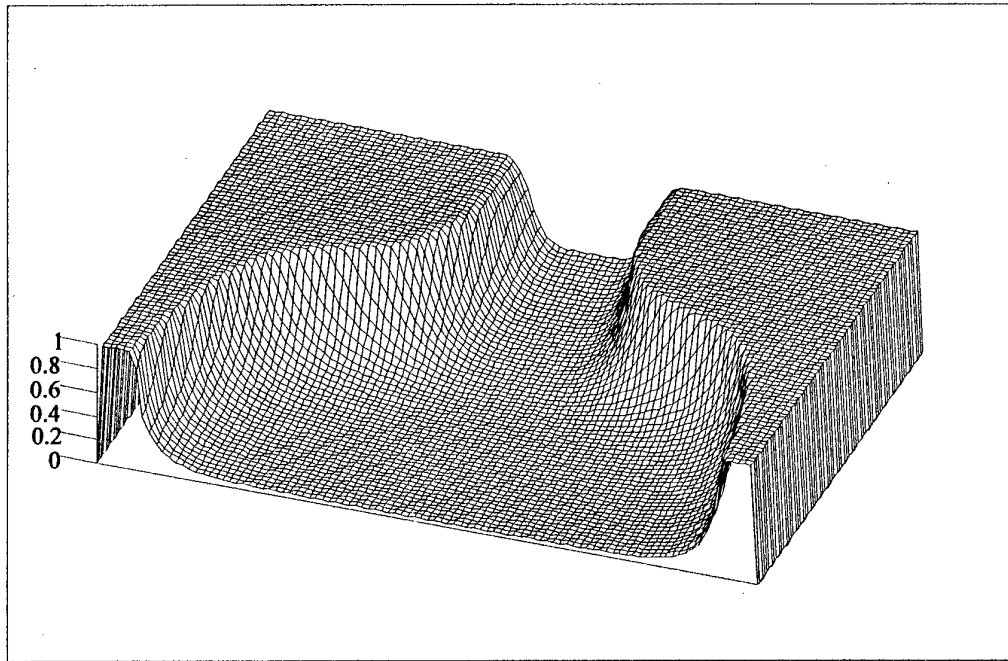
N

Fig.29. A surface plot of space-time distribution of gas density,

$N(z,t)/N_0$, on filament axis

(p=0.25 atm, $E=0.25E_{cr}$=2kV/cm, a=0.07 cm, λ=8.5 cm)

ss

Fig.30.   A surface plot of space-time distribution of electric conductivity,

$\log[4\pi\sigma(z,t)/\omega]$, on filament axis

(p=0.25 atm, E=0.25E_{cr}=2kV/cm, a=0.07 cm, λ=8.5 cm)

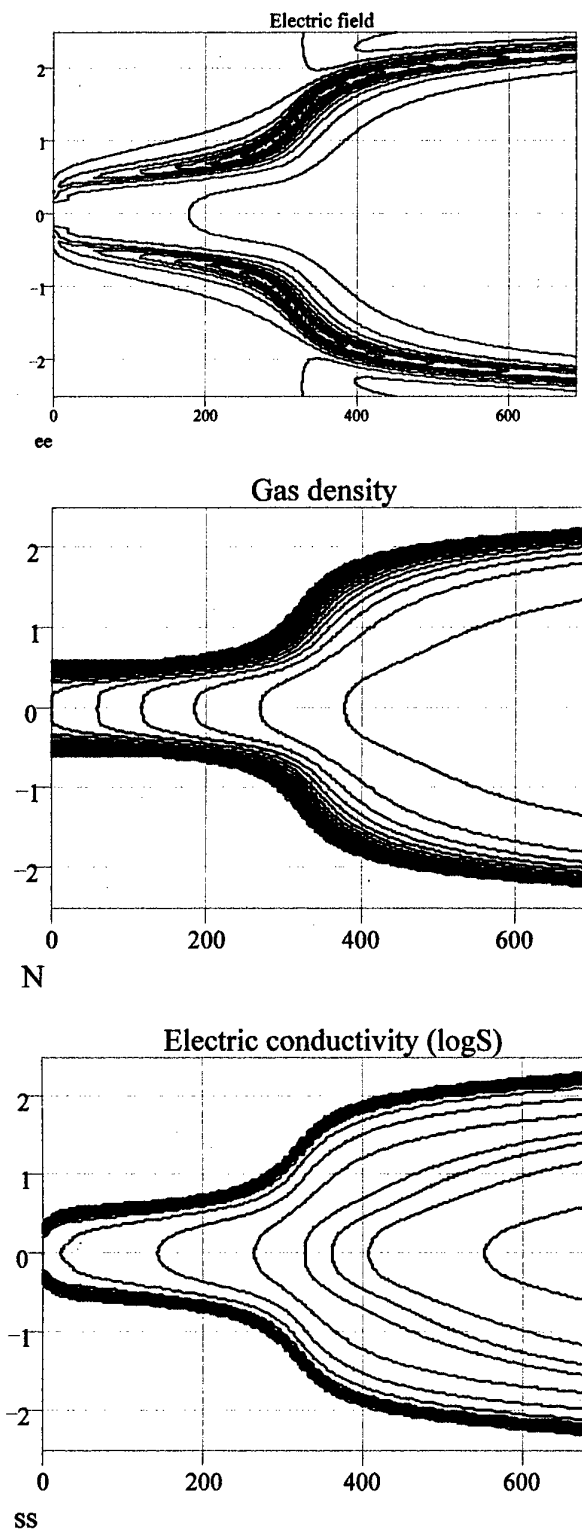Fig.31. Contour plots of streamer parameters

(p=0.25atm, E=0.25E$_{cr}$=2kV/cm, a=0.07 cm, λ=8.5 cm)

kz
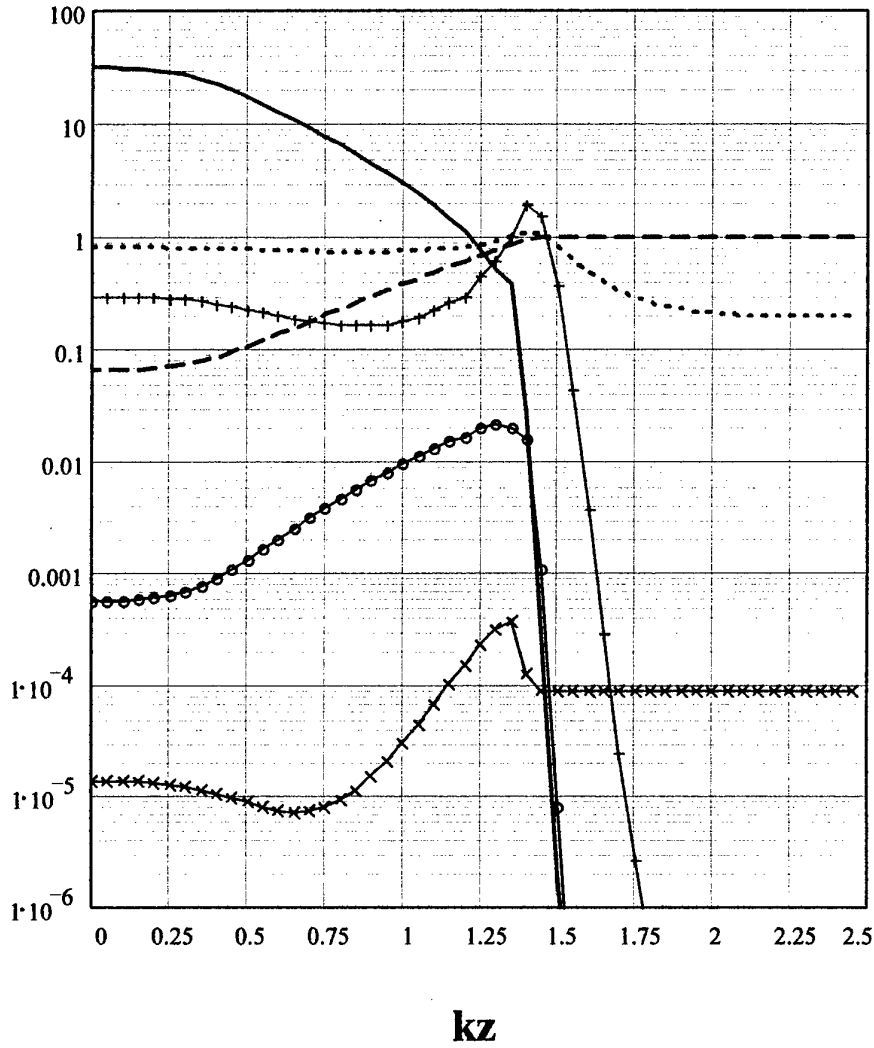
Fig.32. Distributions along filament axis in resonance moment t=13 μs

(p=0.25atm, E=0.25E_{cr}=2kV/cm, a=0.07 cm, λ=8.5 cm).

$\log(4\pi\sigma/\omega)$ – solid line; $|E|N_o/E_{cr}N$ – dotted line; N/N_o – dashed line;

ν_i/ν_{acr} – ++++; $D_{eff}k^2 \cdot v_{ao}$ – xxxx; Q_{heat}/Q_1 – oooo; I_{rad}/Q_1 – boxes
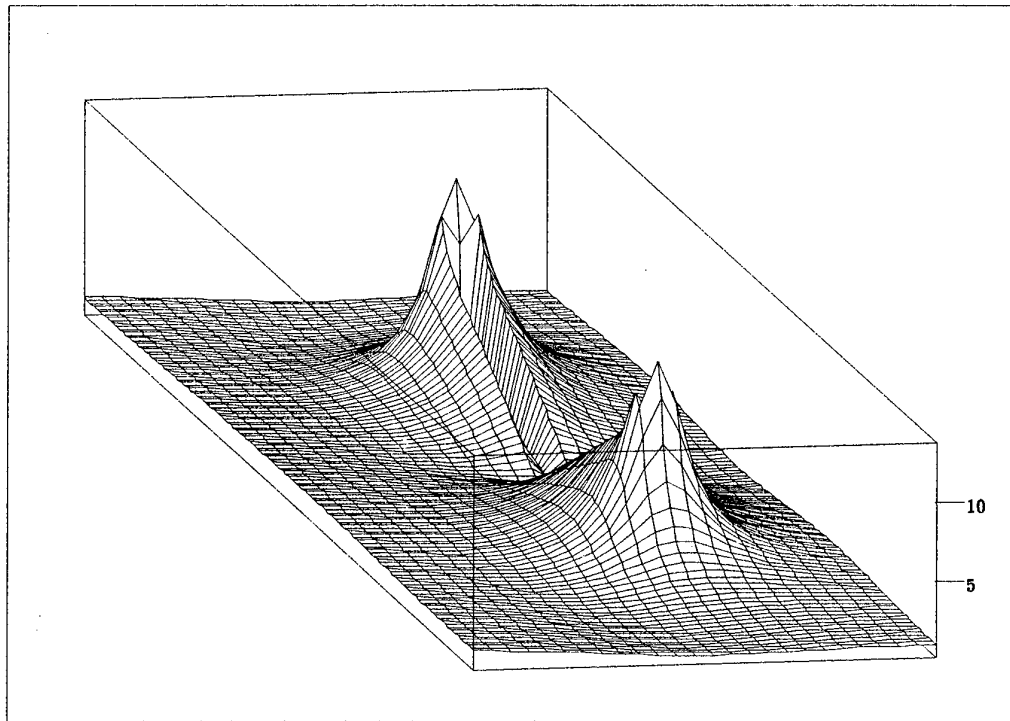
Em

Fig.33. Microwave electric field distribution around a resonant streamer.

The calculated discharge filament velocity and length are similar to that observed.

After resonance achievement the filament does not grow but heating continues. The gas temperature grows up to $1 \div 1.5$ eV along whole filament. The temperature rises slowly when the wave field is undercritical, so isobaric approximation is applicable.

9.3. Discussion

The real phenomenon is much more complicated than the model. The question about streamer radius remains to be open. In frame of usual plasma hydrodynamics one can suggest that the streamer head radius is defined by necessary field growth at the streamer head but it can not be less than ionization avalanche front depth [23]. In a real discharge there are many filaments. Their currents influence one another. The filament placed nearer to the wave radiation source has advantage and shields the filaments situated farther from the source. The shielding effect limits the life time of a filament after arising of the next one.

Let us estimate the average velocity of streamer discharge propagation. The streamers are situated one from another on averadge distance $\lambda/4$ (λ - wave length of microwave radiation). The numerical simulation show that on the ends of a sreamer perturbed electric field approximately equals to critical value:

$$E_{end} \approx E_{cr}.$$

This circumstances give possibility to estimate the average discharge velocity from radiation energy flow (Umov-Poynting vector) and specific average energy needed for heating of streamers

$$<V_{dis}> \approx c \cdot E_o^2 \cdot (\lambda/4)^2 / 8\pi \cdot W \cdot \pi \cdot a^2,$$

where W is internal energy of heated streamer, a - streamer radius. From electrodynamic thin vibrator theory one knows that

$$E_{end} \approx E_0 \cdot \lambda / (c \cdot R \cdot a \cdot \sqrt{2})$$

where R is double radiation resistance. Finally we have for λ=8.5 cm

$$<V_{dis}> \approx 10^6 \cdot p, \; cm/s,$$

where p - air pressure, atm.

This estimation and experimental data are demonstrated on Fig.34. One can see the good accordance. For the conditions of the numerical experiment (p=0.25atm, λ=8.5 cm) estimated propagation speed of a streamer discharge equals $2.5 \cdot 10^5$cm/s. It corresponds to the computational result very well.

The undercritical discharge can exist if the end of one streamer gives the start to another, step by step without interruption. As a result the hot filament net appears.

The large value of discharge speed allow existance of the discharge in supersonic unperturbed flow with M=2.5 if the air pressure less than 0.085 atm.

9.4. Summary

- The streamer discharge generate the thin filaments of hot gas. The resonant streamer is able to absorb the radiation specific power from cross-section equaling the $\lambda^2/4$. The streamer temperature (T>5000K) is enough for ignition of combustion mixture.

- The undercritical streamer microwave discharge propagate velocity is independent on electric field and proportional to the gas pressure.

- The numerical model of a single streamer discharge in microwave radiation is developed. The developed UHF streamer model will be used for more detailed study of streamer behavior at any conditions.
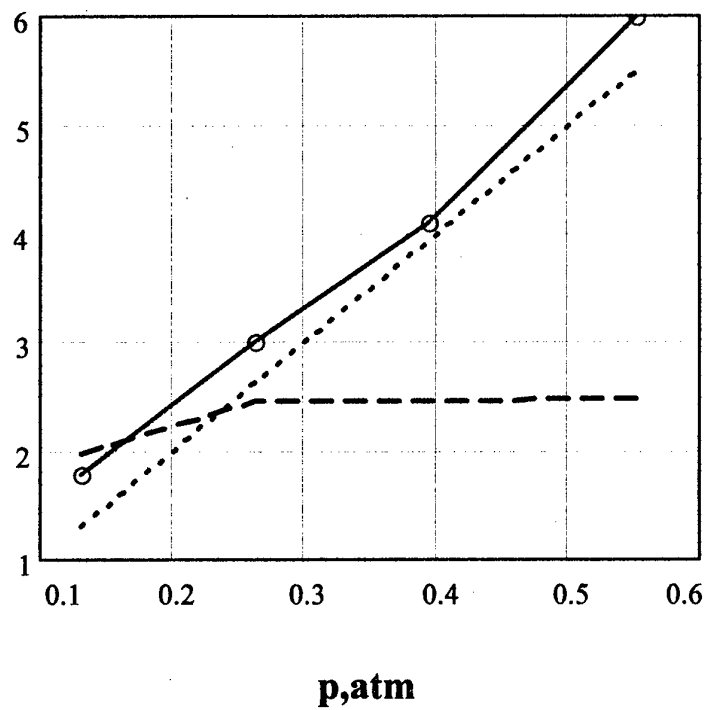
V, km/s

E$_0$/E$_{cr}$

p,atm

Fig.34. The MW discharge propagation velocity dependence upon air pressure.

The experimental data - solid line, estimation – dotted line.

The subcriticality parameter E$_{cr}$/E$_0$ – dashed line.

10. Estimation of Opportunity to Use the Subcritical Streamer
of Microwave Discharge for Ignition of Fuel
in a Supersonic Ramjet Engine

Let us estimate of an opportunity of use of a microwave discharge for ignition of fuel in the supersonic jet engine with use of air as a model gas.

A schematic diagram of such ignition is given on Fig.35. A ramjet flow channel has a radio-transparent window on its wall, for input of the microwave radiation. The microwave beam is focused on the initiating vibrator that is located on the opposite wall. The microwave discharge starts on the initiator (or a set of initiators), shifts up the MW energy flow (towards the radiation source), and fills all the volume of the electromagnetic beam, and ignites a combustible mixture in all the volume. The region of ignition is spatially stabilized by optimization of parameters of the microwave radiation (value of electric field E_o, microwave pulse duration τ, repetition rate of microwave pulses, regime of focusing the beam, etc.).

Let's carry out quantitative estimations. Consider a flight at altitude of 15km (that corresponds to air pressure about 80 Torr), with M = 2 (or with an aircraft speed approximately equal to 600 m/s). In such a case, at an isoentropic airflow in a duct of the ramjet, the compression ratio in the combustion chamber is about 8, and gas molecule concentration there is 4 times as high as in the ambient air, that corresponds to $E_{cr} \cong 13$ kV/cm. At $\Psi = 13$, the field in the electromagnetic beam focal region should be $E_o \cong 1$kV/cm, or $S_o \cong 10^3$ W/cm^2. At wavelength λ=4 cm and at focusing the electromagnetic beam into a spot with a diameter about λ (i.e. with an area about 10 cm^2), the total power of the electromagnetic beam should be about P = 10 kW.
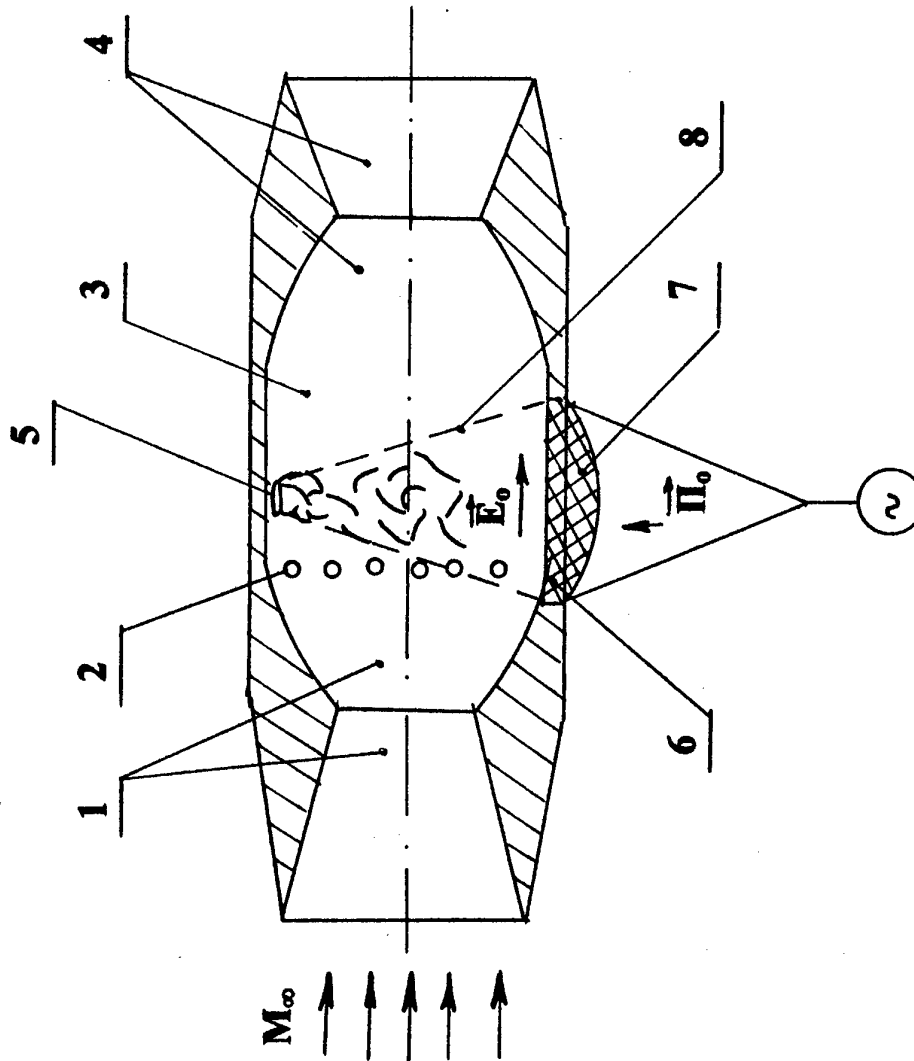
Fig.35. A schematic diagram of fuel ignition in a ramjet with use of an initiated

streamer MW discharge with a developed structure.

1 - a supersonic diffuser; 2 - fuel injectors; 3 - combustion chamber;

4 - a supersonic nozzle; 5 - an initiator; 6 - a radio-transparent window for the

MW radiation; 7 - focusing system; 8 - MW radiation beam

Thus, to provide a continuous ignition in a ramjet, one has to provide an on board electric power supply for P_Σ = 20-50 kW (with account of various efficiency coefficients), that looks quite acceptable.

Note that this value results from estimates for air, real combustible mixtures differ from pure air, that may change kinetics and cause considerable deviations of P and P_Σ.

According to equation (4), under the specified conditions the growth rate of the streamers is equal to 6 10^5 cm/s. It essentially exceeds speed of flow in the combustion chamber of the engine. In this case it is possible to assume, that the flow will not change essentially the microwave discharge character, though the process of ignition under such conditions must be studied specially.

For ignition of fuel in a ramjet it is possible to consider a possibility to use still lower level of field, at which streamer microwave discharges do not achieve the stage of developed structure. To implement it, one can install a grid of thin initiating vibrators near fuel injectors in a combustion chamber, see fig.36. At Ψ > 20 ignition of a combustible mixture will take place only near the vibrators' ends, for the streamers will not leave this region.

In this case the required value of beam power P decreases dramatically – for the conditions of the example considered above it will not exceed several kW. To obtain the value of the optimal, minimal power P, it is necessary to produce experiments with direct MW ignition of fuel.
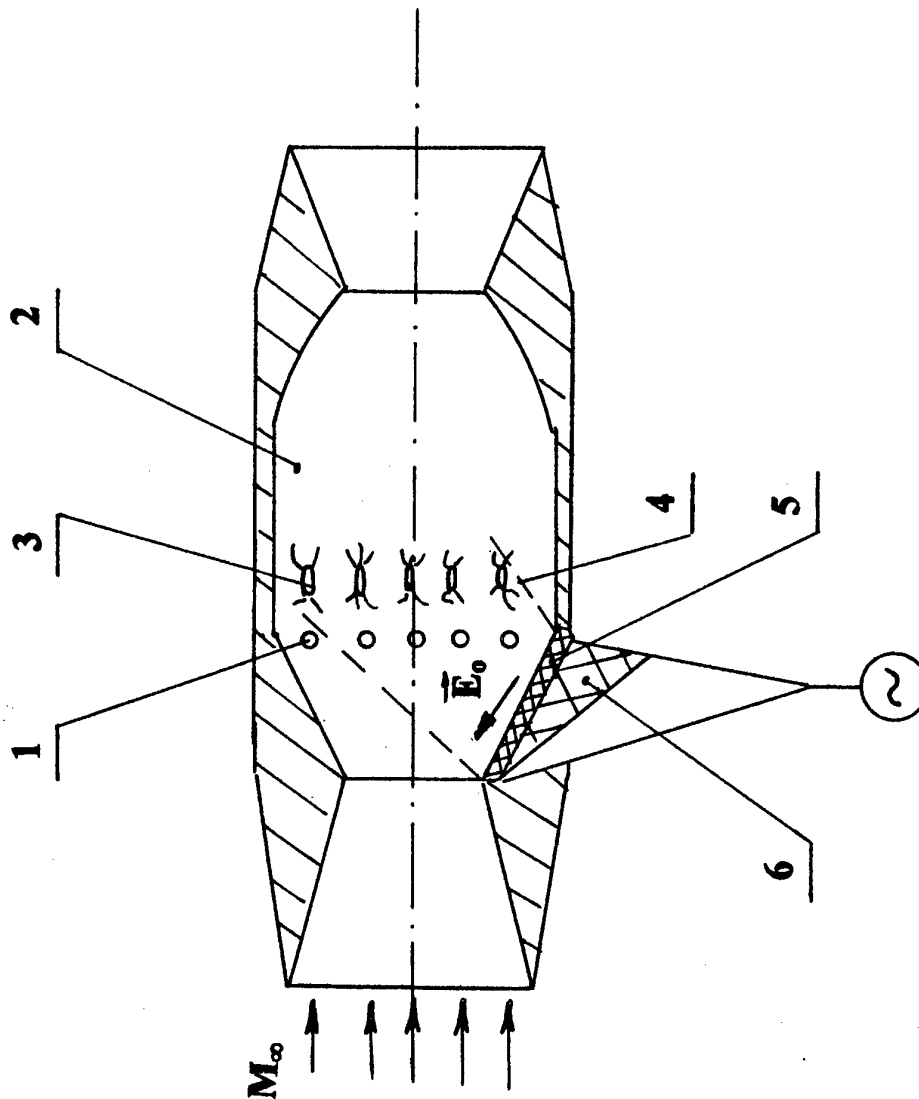
Fig.36. A schematic diagram of fuel ignition in a ramjet with use of a streamer

MW discharge with a high subcriticality

1 - fuel injectors; 2 - combustion chamber; 3 - initiators; 4 - MW radiation beam;

5 - a radio-transparent window for the MW radiation;

6 - a system of the beam formation

11. Conclusions

Thus, our experiments have shown, that the microwave gas discharges under certain conditions proceed in a streamer regime. The MW streamer discharges can exist at electric fields which are essentially lower than the critical breakdown field. Ignition is required to initiate such subcritical MW streamer discharges. These discharges pass serial stages: diffuse, ionization and heating, streamer, and resonant; it is independent of sort of gas.

Under conditions of our experiments the initiated discharges had the developed streamer structure at subcriticality about 20. The temperature of internal areas of the discharge, and especially of their resonant parts, reached several thousands degrees. At the initiated discharges with higher subcriticality and high pressure, streamers were still observed, but they did not part from the initiator - they existed only in the regions with field concentration.

Our estimates on base of results of the researches have shown that there exists an opportunity to use the initiated subcritical MW streamer discharges for ignition of fuel in a ramjet engine at rather a low level of power consumption for generation of the MW beam.

However, one cannot consider the discharge study to be completed, even for air, especially from the viewpoint of its application in aerodynamics. The basic question is its behavior in airflow. It is natural to assume, that the rather a small flow speed of hardly will not change the basic physics of the discharge. However, macroscopic structure may be different. Thus, experiments in supersonic airflow should be carried out.

It is necessary to find out the values of threshold subcriticality of formation of streamers, and the developed streamer structure. It may define the demands for the necessary MW beam power.

For application of the MW discharge for ignition of a combustible mixture, it is necessary to produce experiments just in this vary medium. There should be measured the corresponding threshold conditions of ignition, formation of streamers, and of the developed structure, as well as characteristic rates of discharge processes. And, at last, conditions of ignition must be determined. Experimental results for MW discharges in air and in hydrogen mixture have shown that gas heating rates in combustible gases are much higher. It says that prospects of MW discharges application for ignition of fuel in a jet engine seem to be even more optimistic than they had been considered to be before; whereas simple extrapolation of results of MW discharges in air to MW discharges in air-fuel mixtures is incorrect.

The described above researches of MW discharges in supersonic gas flows can be carried out on base of the experimental installation, which has been used in this work, provided a certain modernization is done. The discharge in a combustible mixture should be studied already at the following stage and, naturally, on the specialized installation.

References

1. L.P.Grachov, I.I.Esakov, K.V.Khodataev et al //The development stages of the electrodeless microwave discharge //Jurnal Tehnicheskoy Fisiki, vol.66, is.7 (1996), p.32-45.

2. L.P.Grachov, I.I.Esakov, K.V.Khodataev et al. Dependence of gas discharge in microwave beam focus evolution on pressure. //Jurnal Tehnicheskoy Fisiki, (1994), v.64, No.1, pp.74-88.

3. L.P.Grachov, I.I.Esakov, K.V.Khodataev et al. Air discharge in quasi optical microwave resonator. // Jurnal Tehnicheskoy Fisiki, (1994), 64, pp.26-37

4. A.S.Zarin, A.A.Kuzovnikov, V.M.Shibkov. Freely localized MW discharge in air. Moscow. Oil & Gas. (1996), 204p.

5. V.V.Zlobin, A.A.Kuzovnikov, V.M.Shibkov. Consentration of electrons in a stimulated MW discharge channel in nitrogen. //Moscow University Physics Bulletin. Fizika, vol.43, No.1, (1988), p.98-100.

6. A.A.Devyatov, A.A.Kuzovnikov, V.V.Lodinev, V.M.Shibkov. The mechanism of molecular gas heating in a pulsed free-localizing RF discharge. //Moscow University Physics Bulletin. Fizika, vol.46, No.2, (1991), p.28-31.

7. L.P.Grachov, I.I.Esakov, K.V.Khodataev et al //The high-frequency air breakdown in presence of vibrator // Jurnal Tehnicheskoy Fisiki, vol.65, is.7 (1995), pp.60-67

8. L.P.Grachov, I.I. Esakov, K.V.Khodataev et al,. High frequency breakdown at metal sphere presence. // Fizika plazmy. (1992), v.18, No.3, p.411-415.

9. Grachov, I.I. Esakov, K.V.Khodataev et al. The front speed of initiated discharge in microwave beam //Jurnal Tehnicheskoy Fisiki, (1995), v.65, No.5, p.21-30.

10. L.P.Grachov, I.I.Esakov, K.V.Khodataev et al. High speed photo registration of

high pressure discharge in microwave beam. //Pis'ma v Jurnal Tehnicheskoy Fisiki, 26 November (1992), v.18, No. 22, ñ. 34-38.

11. K.V.Khodataev. Gas dynamic processes in extra high power high frequency discharge plasma // Proc. of XX International Conference on Phenomena in Ionized Gases, (1991), Italy, Invited Papers, p. 207-217

12. K.V.Khodataev Hydrodynamic processes in the plasma of the extra high power high-frequency discharge // Himicheskaya Fisika, (1993), vol.12, No.3, p.303-315

13. L.P.Grachov, I.I.Esakov, K.V.Khodataev et al. The electrodeless discharge in air under moderate pressure //Jurnal Tehnicheskoy Fisiki, (1985) v.55, No.2, pp. 389-391.

14. L.P.Grachov, I.I.Esakov, et al. The development dynamics of the spatial structure of the electrodeless discharge //Jurnal Tehnicheskoy Fisiki, vol.59, is.10 (1989), p.149-154

15. V.V.Lodinev, V.M.Shibkov, L.V.Shibkova. Gas heating kinetics in pulse-periodic air discharge. //Moscow University Physics Bulletin. Fizika, vol.51, No.2, (1996), p.26-31.

16. A.A.Kuzovnikov, V.M.Shibkov, L.V.Shibkova. Free-localized pulse-periodic MW discharge in air. Kinetics of gas heating. //High Temperature, vol.34, No.3, (1996), p.343-348.

17. G.M.Batanov, S.I.Gritsinin, I.A.Kossyi et al. //Trans. of FIAN USSR. (1985), v.160, pp. 174-203

18. V.M.Shibkov. Free-localized pulse-periodic MW discharge in air. Electric field strength in plasma. //High Temperature, vol.34, No.4, (1996), p.519-524.

19. A.A.Kuzovnikov, V.M.Shibkov, L.V.Shibkova. Kinetics of charged particles in a free-localized pulse-periodic MW discharge in air. //High Temperature, vol.34, No.5, (1996), p.651-655.

20. A.L.Viharev, B.V.Gildenburg, A.V.Kim et /In book "High frequency discharge

in wave fields." IPF AS USSR. Gor'kiy, (1988), pp. 41-135.

21. B.V.Gildenburg , I.S Guschin, S.A.Dvinin et al //JETF, (1990), 94, p.1151

22. K.V.Khodataev, B.R.Gorelik. //Fisika plasmy, (1997), v.23, p.3

23. Pocklington H.C., Camb. Phil. Soc. Proc., 9 (1897). p.324

24. Richmond J.H., Proc. IEEE, 53 (1965). p.796

25. A.W.Ali. //Laser and particle beams. (1988). v.6, part 1, p. 105-117

26. P.H.Purdie and J.Fletcher //Aust. J. Phys., (1992). v.42, p.75-84.

27. A.L.Viharev, L.A.Ivanov, A.N.Stepanov. //In book "High frequency discharge in wave fields." //IPF AS USSR. Gor'kiy, (1988), p. 212-230.

28. S.Brown. //Elementary processes in a gas discharge plasma. Gosatomizdat, (1961), p. 6.

29. Yu.P.Rayzer. //Gas discharge physics. Nauka. (1987), pp. 73, 102, 325.

30. V.A.Rojanskiy, L.D.Tsendin. //Collisionless transfer in partially ionized plasma. Moscow. Energoatomizdat. (1988), p. 26.

Project Principal Investigator   A.P.Ershov

Dr. A.P.Ershov

Department of Physics

Moscow State University

119899, Moscow, Russia

Tel.:   007-095-9391337

Fax.:   007-095-9391787

E-mail: shibkov@ph-elec.phys.msu.su

E-mail: alex@ph-elec.phys.msu.su